Reply to Reviewer 1

General comment:

We thank the reviewer for her/his careful consideration of the manuscript and her/his well thought-out comments, which significantly helped to improve the paper. In the following, we address all comments and questions raised (Reviewer's comments in italics). Text changes in the manuscript are highlighted in red (except minor wording changes). Main changes concern: (i) an extended discussion of the evolution of the PV-gradients and the related transport barrier over the season and potential relations to convective activity (including ozone, mean age, OLR and diabatic heating rates in the revised Fig. 12) in section 5, (ii) a critical discussion of the leakiness of the diagnosed barrier (discussion), (iii) an extended discussion of MLS observations and the comparison between model and MLS (discussion, including a new Fig. 14), and (iv) shifts of the old section 6 to the appendix, of the discussion of the layer where our criterion is applicable to section 4, and of the discussion of the anticyclone location probability to the new section 6.

Issue 1: *The authors have done a wonderful job of describing their analysis with examples from a particularly good case that occurred July 6 2011. They have also performed analysis over 3 summer seasons as demonstrated by Table 1 and Fig. 11 (although this figure only shows 1 season). However, the paper relies too heavily on the July 6 analysis. This applies to the discussion of Figs. 3, 12, and 13 that should, in my opinion, relate seasonal data and not just values from 1 day. Fig. 3 is important because it demonstrates that results from CLaMS (the transport model) agree with MLS data. The agreement between models and satellite data can be very fickle; one might get great agreement one week and terrible the next. It is therefore important to provide the reader with a more thorough indication of how good the agreement actually is. For the early figures, it is appropriate to focus on July 6. The analysis afterward (Figs. 11-13) is essentially a demonstration of how good the barrier model is and should not be restricted to July 6. However, after showing seasonal data in Fig. 11, the authors return to the July 6 analysis for Fig. 12 and 13. I think that these figures should show seasonal results. In addition, Fig. 11 should have two more panels: one for O3 and one for age of air.*

The reason to focus on one single day (6 July 2011) for large parts of the paper was to describe the methodology as simply and clearly as possible. However, as Reviewer 1 (and also Reviewer 3) points out, the discussion of how "good" the diagnosed barrier is, should not be restricted to this single date. Indeed, we showed seasonal data already in the draft for the PV-gradient and CO-gradient (old Fig. 11). This figure now includes also ozone and mean age, as suggested by the Reviewer. Furthermore, we now present the ozone-gradients from MLS for the entire summer season (new Fig. 14), and discuss the agreement with the CLaMS model and possible shortcomings in Sect. 5. Comparison of tracer maps shows good agreement between CLaMS and MLS ozone and CO throughout the summer, similar to the case in Fig. 2 (see also Pommrich et al., 2014). Concerning the gradients, good agreement is only found for parts of the season (beginning and mid-end of July). However, the disagreements in the exact location of maximum gradients (e.g., during August) are not unexpected, due to very different resolution of the model and MLS observations (e.g., the model has a vertical resolution of about 400m around the tropopause, whereas MLS has about 3 km). This fact demonstrates the need for high resolution measurements in the Asian monsoon region.
The characteristic of the transport barrier to be best detectable at 380 K holds for the whole summer season. However, we think that showing plots like Fig. 11 (old version) also for other levels than 380 K would overfill the paper with unnecessary material. Therefore, we kept the old version of Fig. 13 (old version), but present the respective part at an earlier place in the paper (end of section 4).

Issue 2: *This issue concerns the use of the term barrier. This term is widely used in the literature and, so, I understand why the authors might choose to use it as well. However, I think it is misleading and the maps in Fig. 9 seem to support this contention. I would prefer it if the authors referred to the PV gradient as a diagnostic of how strong (or weak) cross-gradient transport is likely to be the stronger the PV gradient, the weaker cross-gradient transport is. The reason that the term barrier is not appropriate is because it invokes the concept of an external restriction on the flow (e.g., a wall) and of causality. However, PV and cross-gradient transport are both merely related properties of the circulation; they are highly correlated but neither causes the other to occur.*

We totally agree with the Reviewer's view. However, we would keep the term "barrier", which is indeed usually used in the literature as Reviewer 1 also remarks, to have some simple terminology. We discuss the term "barrier" now briefly at the end of the introduction and more extensively in the discussion (see also our reply to Reviewer 2/Major comment 1).

Specific and technical comments:

Page 10594, line 25: *Regarding the linear response . . .. One obtains a strong anticyclone over Asia as the linear response to low-level convective heating associated with the Asian monsoon. However, the anti-cyclone has nonlinear components. I suggest rewording the is sentence to reflect that fact.*

Sentence has been reworded!

Page 10595, line 5: *Remove characterized.*

Done.

Page 10595, lines 24-25: *Here and throughout the text, the authors use has been where was is appropriate. Has been should be used when something started in the past and continues into the present. In this particular case, the use of PV gradients originated at a particular time in the past it is not continually being originated. Change has been to was.*

We corrected all cases pointed out by the Reviewer and carefully checked the text again for further mistakes.

Page 10595, line 26: *Change In fact, the to This*

Done.

Page 10595, lines 26-27: *Change relies on the characteristics of PV being an approximately conserved quantity to relies on the fact that PV is approximately conversed*

Done.

Page 10597, line 2: *Change for suppressed to of suppressed*

Done.

Page 10597, line 2: *Change has been to was*

Done.

Page 10597: *Age of air should be defined here. Section 3: Why not show CO from MLS?*

Age of air is defined now - Thanks for pointing this out to us. MLS CO has a worse vertical resolution (about 4.5km) compared to MLS ozone (about 3km), in the region of interest. As the transport barrier is only detectable in a small vertical layer around the tropopause, MLS ozone is clearly advantageous over MLS CO for our purpose. This is stated now at the end of Sect. 2.

Page 10599, lines 10-11: *Change has been to was*

Done.

Page 10599, line 16: *Change has been to was*

Done.

Page 10600, line 5: *Change has been to was*

Done.

Page 10600, line 8: *Change barrier of the subtropical jet to barrier for the subtropical jet*

Done.

Page 10600, line 14: *Change has been to was*

Done.

Page 10600, line 16: *Change change of our results to change to our results*

Done.

Page 10600, line 17: *Change In analogy to to Following*

Sentence changed, as suggested by Reviewer 3.

Page 10600, line 18: *Delete in the following (within parentheses)*

Done.

Page 10601, lines 27-28: *The statement that barrier is located . . . in the latitude range of decreasing circulation seems to contradict Fig. 7, which shows that circulation increases with equivalent latitude. Please clarify.*

This sentence was indeed written unclear. We meant to say that the barrier needs to be located in the region where the circulation decreases when moving away from the anticyclone center (hence, with decreasing monsoon equivalent latitude). The sentence has been reworded.

Page 10604, line 19: *Change has been to was*

Done.

Reply to Reviewer 2

General comment:

We thank the reviewer for her/his careful consideration of the manuscript and her/his well thought-out comments, which significantly helped to improve the paper. In the following, we address all comments and questions raised (Reviewer's comments in italics). Text changes in the manuscript are highlighted in red (except minor wording changes). Main changes, related to all Reviewers's comments, concern: (i) an extended discussion of the evolution of the PV-gradients and the related transport barrier over the season and potential relations to convective activity (including ozone, mean age, OLR and diabatic heating rates in the revised Fig. 12) in section 5, (ii) a critical discussion of the leakiness of the diagnosed barrier (discussion), (iii) an extended discussion of MLS observations and the comparison between model and MLS (discussion, including a new Fig. 14), and (iv) shifts of the old section 6 to the appendix, of the discussion of the layer where our criterion is applicable to section 4, and of the discussion of the anticyclone location probability to the new section 6.

Major comments:

1. *As previous studies have shown, Ertels PV and long-lived tracer distributions are highly correlated in their spatial and temporal distributions inside the Asian monsoon anticyclone. I dont necessarily think the PV as a barrier but as a measure of confinement of the air masses within the anticyclone. This barrier is leaky and also has large variability, if it exits. The authors also have introduced three other variables to characterize the monsoon anticyclonic boundaries in section 2, which include, PV, circulation and stream function. With this in mind, the authors have to emphasize if it is possible to define a barrier over the monsoon region. Maybe there is no barrier? Why using PV gradients defining the transport barrier following Nash et al. (1996) over the monsoon region is applicable and what that means physically. Also, as the magnitude of PV is highly dependent on altitude, it will be useful to use MPV (modified PV) instead of PV and show how the results will change.*

We agree with the Reviewer's view that there is some transport across PV-contours and that the enhanced PV gradient in the monsoon region is better interpreted as a measure of confinement than as a rigid barrier to transport. We note and discuss this now more critically at several places in the manuscript (e.g., end of introduction, discussion). However, we keep the term "barrier" for sake of having a clear terminology (and because of its frequent use in existing literature).
As our analysis is carried out on surfaces of constant potential temperature using a modified PV by scaling with a θ-dependent function, as used e.g. by Randel et al. (2006), would cause no change to PV-gradients and therefore to the fact whether amaximum gradient emerges or not (only the corresponding PV-value would change). To keep things as simple as possible we therefore don't introduce modified PV.

2. *The 380 K isentropic surface can well be representing the dynamic variability of the Asian monsoon anticyclone in the tropics and subtropics. However, as shown in the previous studies, the transport processes near the Asian monsoon region are occurring in the thick layer instead of on a surface. In fact, 360 K can be a better representative of the Asian monsoon anticyclone itself (where both the jet streams act as a boundary, see Fig. 1). Even though the transport barrier defined in this study is most distinguishable at 380 K surface, I think it is important to emphasize how the entire monsoon system has rather a layered structure and the method used in this study is subjective to the PV values itself. For example, based on Fig. 13 one can probably define transport barriers at 370 and 390 K as well based on smaller PV gradients over different equivalent latitudes.*

Indeed, maximum PV gradients can be found also at 370 and 390 K, as discussed in relation to Fig. 8 (already in the submitted version). This part has been moved to Sect. 4 in the revised version, to have its discussion at an earlier place in the paper. Moreover, we extended this paragraph to include now also a brief discussion about the layered structure of the monsoon system.

3. *Defining polar vortex edges, as in the previous studies, can be useful in knowing polar vortex breakdown dates and so on. Then how is the definition of transport barrier in the Asian monsoon anticyclone based on PV gradients useful? For example, can this diagnostics be used in quantifying vertical transport from the upper troposphere to stratosphere or size of the anticyclone? Are the characteristics of the transport barrier affected by the convective activities in the lower troposphere and the strength of vertical and horizontal circulations near the monsoon region? I think the importance (and usefulness) of defining anticyclonic transport barrier based on PV gradients has to be emphasized in a broader context in relation with dynamical and chemical variabilities of the monsoon anticyclone and convection.*

For understanding the details and exact mechanisms of Asian monsoon transport into the lower stratosphere (e.g., of pollution) it is indeed important to know the degree of confinement inside the anticyclone. As shown in recent studies, the anticyclone is composed by air masses originating from different pathways, like upward transport inside the anticyclone core (Bergmann et al., 2013), or injection into the anticyclone edge by taifoons (Vogel et al., 2014). The mixing between these air masses and hence chemical reactions and lifetimes will depend on the degree of isolation of the core from the edge region. Furthermore, knowledge of the anticyclone core (inside the PV-barrier) offers a method to determine the anticyclone size and to tag air masses which are inside the anticyclone. This offers new opportunities for model studies as well as for the interpretation of measurements. A new paragraph in the discussion focuses on these issues.
Defining exact onset and breakdown dates of the anticyclone by using the determined PV-barrier seems problematic to us, because the anticyclone needs to be sufficiently strong for the PV-barrier criterion to hold. Hence, confinement of trace gases inside the anticyclonic circulation becomes evident from visual inspection of tracer maps already 1-2 weeks before the barrier can be determined. Likewise, when the anticyclonic circulation weakens tracer anomalies in the monsoon region remain a few weeks after the last date with a clear PV-gradient maximum. These issues are described and discussed now in Sect. 5.
For a more appropriate discussion of the relation between the transport barrier characteristics and convective variability, we now include timeseries of OLR and integrated diabatic heating rate (as proxies for convection) in Fig. 12. During end of July, the variability in the barrier and the related disagreement between PV- and CO-gradient maxima appear to follow strong convective activity with a lag of about a week, similar to the time lag between the anticyclone response and convection as found by Randel et al. (2006). Also during beginning of July and mid-end of August the increase in the barrier PV-value seems to follow strong convection. The significance of this observation and the detailed mechanism involved need to be further studied. We discuss these issues now in Sect. 5 in relation to Fig. 12.

Minor comments:

P1, L59 *is $\rightarrow$ and is*

We think this would change the meaning of the sentence and therefore we keep the old version. Please correct us if we are wrong!

P1, L60-67 *It should be mentioned that why those simple methods are problematic or unsatisfactory and also how it affects the results of various diagnostics (related to major comment ♯ 1).*

The sentence has been slightly extended, and together with the extended discussion about the usefulness of determining the transport barrier (see reply to Issue 3) hopefully clarifies these issues.

P1, L68 *What does physically motivated mean?*

“Physically motivated” here should mean that the PV-gradient related transport barrier is based on conservation properties of the flow. The sentence has been extended.

P2, L93 *We interpolated... $\rightarrow$ What are the reasons for the horizontal interpolation and also what is the original grid of the ERA-interim data?*

The formulation in the submitted version was not correct - thanks for pointing this out! We used the ERA-Interim data on the $1^\circ \times 1^\circ$ horizontal grid as provided by the ECMWF and interpolated it only in the vertical.

P2, L57 *in the monsoon $\rightarrow$ in the monsoon anticyclone*

Done.

P2, L150 *At the end of this paragraph, a brief comment about CLaMS CO and ozone reproducing climatology and/or observations will be helpful.*

The description of CO, ozone and mean age in the model has been extended, including appropriate references showing comparisons with observations in the UTLS.

P3, L176 → *model and simulations → model simulations and the satellite observations*

This formulation was indeed nonsense - Thanks for pointing this out! Sentence has been changed.

P3, L202 *What are the boundaries of the Asian monsoon region here?*

This information was included in the caption of Fig. 3 (10°N-60°N and 10°W-160°E). We include it now also in the main text.

P3, L232 - *-10E → 10W?*

Changed!

P4, L320- 325 *This is an interesting point. As the anticyclone itself wont disappear during this period, one can argue that this PV gradients-based method fails locating the transport barrier. Do the actual PV values and tracers maxima show clear boundary of the anticyclone during this period? Or the anticyclone is simply too weak to act as a transport barrier?*

Trace gas confinement inside the anticyclone (at 380K) can be seen already 1–2 weeks before the PV-gradient maximum clearly emerges, and remains also longer than the barrier may be determined. Our interpretation is that the anticyclonic circulation and the related confinement need to be sufficiently strong that the PV-gradient barrier criterion in the monsoon holds. This is more clearly discussed now in Sect. 5 and in the discussion (Sect. 7).

P5, L380-383 *Is there any possible explanation to this feature?*

See our response to Major comment 3.

P5, L459 *Also, there is a possibility that the monsoon anticyclone is not as isolated as the polar vortex or the jet stream.*

Indeed, we think this is the case! We significantly changed the whole discussion paragraph with the aim to clarify things.

P6, L548-550 *More specific information about how this can be done?*

We included a new paragraph about the usefulness of the determined transport barrier in the discussion (see our reply to Major comment 3), and also briefly refer to this discussion here.

P7, L685 *This citation year needs to be corrected from 2006 to 2007.*

Corrected!

P9, Fig. 2c *The wind vectors are hard to see in this plot. Using slightly darker grey color should help. . P9, Fig. 4 I have a feeling that the map projection underneath the PV contours is not correct. The secondary PV minimum on the left hand side should sit somewhere in the Middle East not over North America or Pacific (see Fig. 10 of Garny and Randel, 2013).*

Wind vectors in Fig. 2 are in darker grey now. Regarding Fig. 4 we cross-checked that the secondary PV minimum at 380 K on 6 July 2011 is indeed located above Northern America, and is related to Rossby-wave breaking occurring there on this particular day. Interestingly, at 360 K there is an additional PV minimum over the Middle East (as in Garny and Randel, 2013) also on this day, which is not detectable at 380 K.

P14, Fig.11b *The crosses in this plot rather look like asterisks on top of filled circles, which make it harder to distinguish from the black diamonds. I would recommend using crosses or pluses in grey colors. Also related to this plot, I wonder why this method works the best in early July. If this method were going to be more practical, I would think it should work from the onset to the end of the summer monsoon.*

We changed the symbols in the figure (new Fig. 12) to improve the presentation quality. The discussion of the evolution of the PV-gradient maximum is now extended, including potential relations to convective activity (see

reply to major comment 3).

Reply to Reviewer 3 (Gloria Manney)

General comment:

We thank the reviewer Glora Manney for her careful consideration of the manuscript and her well thought-out comments, which significantly helped to improve the paper. In the following, we address all comments and questions raised (Reviewer's comments in italics). Text changes in the manuscript are highlighted in red (except minor wording changes). Main changes, related to all Reviewers's comments, concern: (i) an extended discussion of the evolution of the PV-gradients and the related transport barrier over the season and potential relations to convective activity (including ozone, mean age, OLR and diabatic heating rates in the revised Fig. 12) in section 5, (ii) a critical discussion of the leakiness of the diagnosed barrier (discussion), (iii) an extended discussion of MLS observations and the comparison between model and MLS (discussion, including a new Fig. 14), and (iv) shifts of the old section 6 to the appendix, of the discussion of the layer where our criterion is applicable to section 4, and of the discussion of the anticyclone location probability to the new section 6.

Overall comments:

1. *Much of the analysis is focused on 6 July 2011. Why was this particular date chosen? How representative are this date and this year of the Asian monsoon anticyclone conditions in general?*

The 6 July has been chosen as an example of a distinct anticyclonic pattern in PV and several trace gas species and a clear PV-gradient maximum. It is indeed one of the better dates for application of the PV-gradient criterion, although not the best. Figure 12 shows that a similarly clear PV-gradient maximum can be determined for many days during summer 2011. In this sense the 6 July can be regarded representative for air mass confinement during the main monsoon period with a strong anticyclone.

2. *After showing the MLS ozone in comparison with the CLaMS data in Figure 2, the ensuing analysis is done entirely with the model data. For the method to be most valuable, it would be nice to demonstrate more directly that it is useful for analysis of "real" data such as those from MLS as well as for the model dataset. Part of this would be demonstrating more thoroughly the degree of agreement between MLS and CLaMS. Specifically:*
a. *Why not show MLS CO as well as MLS ozone in Figure 2? This would be especially valuable since the ozone chemistry in the ASM anticyclone can be complicated [e.g., Lawrence and Lelieveld, 2010], and thus it may not always be a good tracer of transport.*
b. *In conjunction with (1), how representative is the agreement between MLS and CLaMS around 6 July 2011 of that at other times?*
c. *What is the vertical resolution of the model? The MLS v3 ozone vertical resolution in the UTLS is about 3km is the model really that much better? (Values for vertical resolution for both should be given in the data description.)*
d. *Because the MLS data are time-averaged, one would expect some smoothing out of extrema, which might also contribute to the MLS ozone showing higher minima in the ASM anticyclone (which is where that apparent bias between MLS and CLaMS is most apparent). For the purpose of the comparison, why not time-average the CLaMS data as well and/or interpolate it to the MLS locations and average it in the same way as for MLS?*

We agree that a more extended comparison with observations would significantly increase the value of the determined transport barrier. However, a main problem when comparing to existing satellite measurements is the density of the sampling and the coarse vertical resolution. If the sampling is not frequent enough and data points over a long period have to be collected and averaged to reach a suitable coverage of the monsoon region, the large variability of the anticyclone spoils the barrier calculation as very different dynamic situations are mixed together.
Furthermore, because the PV-gradient maximum can be determined only in a shallow layer around the tropopause (around 370–390 K), a very good vertical resolution of the data is necessary. The vertical resolution around the tropopause in CLaMS is about 400 m. MLS ozone has a vertical resolution of about 3 km, which is significantly lower than the model resolution. Nevertheless, MLS ozone shows maximum gradients coinciding with the PV-barrier for several days during summer 2011. MLS ozone gradients are now presented for the entire summer season in the new Fig. 14. Given the large differences in vertical resolution between CLaMS and MLS, we think this partial agreement is encouraging and provides further confidence in the meaningfulness of the PV-gradient maximum as a measure of confinement (see also reply to Reviewer 1/Issue 1). Vertical resolution of CLaMS and MLS are now given in Sect. 2, as suggested.
MLS CO has a worse vertical resolution than ozone, of about 4.5 km. Mapping MLS CO versus PV (as done for MLS ozone in Figs. 2/14) generally yields very noisy maps and no clear gradient maximum. Therefore, we

decided to focus on ozone. Satellite observations of a better vertical resolution (about 1 km) and an, at least, similar frequent sampling than MLS would be highly advantageous for the analysis of confinement inside the anticyclone. At the moment, MLS provides the best data source.
Indeed, agreement between CLaMS and MLS maps (as in Fig. 2) could be improved if the model data was treated in a similar manner to the satellite data (e.g., mapping to MLS locations and applying averaging kernels). This procedure had been applied recently to CLaMS water vapor (Ploeger et al., 2013) and CLaMS CO (Pommrich et al., 2014). Because for the gradient analysis a frequent sampling and a high vertical resolution are prerequisite, we refrain from applying this procedure here and from degrading the model data.

Specific comments:

-p10594, *is the monsoon circulation really "strictly in the TTL"? It can extend to around 40N, which seems at least subtropical?*

We here followed Fueglistaler et al. (2009) who relate the monsoon systems to the TTL. We think this is a reasonable picture as the monsoons are very relevant to upward transport in the tropics, related to convection and upwelling. However, this is no strict definition and we reworded the sentence slightly.

-p10596, L7: *This section contains a lot of (useful) tutorial material not typically found in "data and model" sections. A more appropriate section title might include "methods" or "analysis" or some similar word. Also, the MLS data used in the paper should be described in this section.*

All suggestions have been adopted.

-p10595, *and subsequently in the paper: Numerous studies in addition to Nash et al (1996) have used PV gradients to define the edge of the polar vortex and assess the strength of its transport barrier (e.g., Manney et al, 1994, GRL there are many others, this is just one that comes immediately to mind, not necessarily the best or earliest). The method that Nash et al introduced was to use the PV gradients constrined by being near a windspeed maximum. Since that windspeed constraint is not being followed here, the method does not "follow Nash" (as is said later in the text), and it would be appropriate to indicate that the PV gradient has been used extensively in this manner both before and after Nash et al.*

We agree and therefore reworded all corresponding sentences, presenting more references and avoiding citing only Nash et al. (at least with an "e.g.").

-p10596, L16: *The ASM region is more subtropical than tropical; therefore 100hPa is closer to 390K in the ASM region.*

Indeed, 100 hPa is located between 370 and 380 K in the core region of the Asian monsoon anticyclone. However, we think that 380 K and 100 hPa are close enough to keep the formulation as is.

-p10599, L4-5: *Doesnt the agreement depend to so extent on the selection of contours? How were the PV and Montgomery stream function contours that are shown chosen? Certainly, the higher Montgomery streamfunction contour shown is obviously irrelevant to defining the anticyclone region. But mightnt a Montgomery stream function contour in between the two lower ones shown do a better job of "outlining" the main anticyclone features?*

The advantage of Montgomery stream function is that it is a much smoother quantity in the monsoon region than PV. However, small-scale variations of trace gas mixing ratios along the anticyclone edge are much better captured by PV. In particular the shedding of the smaller eddy to the east on 6 July 2011 can be clearly seen in PV but not in Montgomery stream function contours, which don't show an isolated eddy. We carefully checked that including more contours does not improve the agreement between trace gas and Montgomery stream function contours. Regarding this better agreement of trace gas confinement with PV than Montgomery stream function, the 6th of July is representative for the entire summer season. We would like to keep the few selected contours for the sake of clarity of the figure.

-p10599, L6-9: *Do the MLS data resolve such small-scale eddies? If not, how is the reliability and accuracy of such fine-scale structure in the model assessed? That is, are we confident that these are "real" features?*

As much of the small-scale variations are only visible in the higher resolution model data and not in MLS observations, it is difficult to proof that these are indeed realistic. However, as the MLS sampling is still not frequent enough to be comparable to the horizontal model resolution (about 100 km) and the vertical resolu-

tion in MLS (about 3 km for ozone, 4.5 km for CO) much coarser than in the model (about 400 m around the tropopause) it is not surprising that the model shows smaller scale features than MLS. Recent comparisons between CLaMS and MLS water vapor (Ploeger et al., 2013), MLS ozone (e.g., Konopka et al., 2010), MIPAS mean age (Ploeger et al., 2015), and various in-situ observations (e.g., Konopka et al., 2007) show that the model generally simulates the observations, and even small-scale variations therein, well. To achieve more confidence in these small-scale features, high-resolution in-situ observations from the Asian monsoon region would be highly beneficial, but these are not existing hitherto. We slightly extended the related discussion paragraphs in Sect. 2 and Sect. 7.

-p10600, L11: *Isn't 10N a little close to the equator to be sure of eliminating all effects of low equatorial PV? Some of the figures seem to show well-separated low PV values at the lower edge of the plots.*

Indeed, there may be some equatorial low PV-values included in the selected monsoon region. But also shifting the low latitude boundary to 15°N would not entirely solve this problem, and further exclude some of the high PV values at the equatorial edge of the anticyclone. Therefore, we decided to use 10°N, but checked that 15°N does not change our results substantially.

-p10600, L17: *See comment above re Nash et al.*

See our reply to the previous comment.

-p10601, L13: *What is the reasoning behind the choice of 30% as the threshold by which the maximum must exceed the minimum?*

This choice is indeed somewhat arbitrary. By visual inspection of the PV($\phi_{\mathbf{eql}}$) function we chose 30% in order to count only clear maxima. For a single date the existence of a PV-barrier could depend on the exact percentage value. However, 30% turned out to be a value with only a very few number of such critical dates, when slightly varying the percentage value. The main conclusion of the paper, that a maximum in the PV-gradient exists and is related to the confinement of trace gases, would not change when using another percentage.

-p10601, L29: *Shouldnt this be "Equivalent latitudes *higher* than the minimum circulation?*

The formulation in the submitted manuscript was wrong (see also our reply to Reviewer 1). We reworded the sentence.

-p10602, L7: *Using "the maximum" here is rather sloppy language, since the largest maximum (and hence "the" maximum if you allow only one) is always that associated with the subtropical jet.*

We reformulated the sentence (e.g., using "local maximum").

-p10602, L11: *Shouldnt this be "at PV values *smaller* than 5 PVU"?*

Yes, indeed - thanks for noticing this mistake!

-p10602, L17: *"enhanced dynamic variability" seems a bit vague many sorts of dynamic variability exist that do not weaken transport barriers.*

We compare the transport barrier evolution to OLR and heating rates now (see new Fig. 12), and find some indication for co-variations with convective activity (see our general comment (i), the new discussion of Fig. 12 and also our reply to Reviewer 2). The respective paragraph here has been reworded.

-p10603, L1-8: *While the agreement between CO and the selected PV contour does appear to be good overall, I think the current text does overstate it somewhat for example, on 2011-07-09, 2011-07-18 and 2011-07-21, some of the highest CO values extend outside the PV contour, and the "split" on the last day is not obvious in CO. It would be more accurate to soften the statements here, and I do not believe this detracts from the message of the paper.*

We agree that the agreement between PV and CO was slightly overtstated in the text. The paragraph has been extended to discuss also disagreements in the Figure. Just a side note: the split on 2011-07-21 can be seen also in CO, but is somewhat hidden in the two highest values of the color code (red and dark red), and

not well visible in the figure.

-p10603, L20-21: *Does the 20 June to 20 August period cover the entire period for which human inspection of the fields (i.e., looking at maps) shows an obvious signature of the ASM anticyclone in CLaMS and MLS trace gas fields? If not, how long are the periods before/after when there is a signature in the trace gases but (presumably) the transport barrier is not strong enough to detect using this method? The CO field in Figure 11 doesnt show an obvious disappearance of that signature at the beginning or end of the plotted period.*

Confinement in trace gas mixing ratios inside the anticyclone is visible from mid June until mid-end September, hence already 1–2 weeks before a clear PV-gradient maximum develops. Hence, the confinement needs to be sufficiently strong for a clear PV-gradient maximum to be detectable. After the last date when the barrier criterion holds, it takes a few weeks until the confinement really vanishes and the mixing ratio anomaly is mixed away (see also our reply to Reviewer 2/Major comment 3). We include a discussion of these issues now in Sect. 5.

-p10604, L2-3: *Figure 11 does show high CO gradients at PV higher than that at the PV gradient maximum for a few days in early and late July, not "only after 15 August".*

We agree that our discussion of Fig. 11 was not satisfactory. We include more tracers (also ozone and mean age) and also proxies for convective activity (OLR, integrated heating rates) now in the revised version of the figure (new Fig. 12). The related discussion in Sect. 5 has been substantially changed (see also our replies to Reviewer 2/Major comment 3 and to Reviewer 1).

-p10604, L8-10: *It is interesting that both 2012 and 2013 show low minimum PV values for the transport barriers than 2011 can you say anything about what this might imply in terms of differences in the ASM circulation?*

We did not analyse the differences in the meteorological situation between different years carefully, except visual inspection of daily maps and calculation of the PV-gradient maxima. A more detailed analysis of the interannual variability would indeed be very interesting and will be the subject of ongoing research.

-p10604, L23: *There are numerous studies besides Sparling (2000) that use PDFs to look at transport and transport barriers: McDonald and Smith (2013) and Hegglin and Shepherd (2007) would be good places to start looking for references. At the very least, add an "e.g.," in front of "Sparling".*

As the discussion of the use of PDFs for studying the transport barrier should not be the focus of the paper and to improve the readability, we moved the respective section to the appendix. The respective text part has been reworded.

-p10605, L7-11: *This is another place where using MLS trace gas data as well as CLaMS to construct the PDFs might be informative and provide insight as to how well the method applies to real data.*

We include an analysis of MLS ozone for the entire summer season now in the discussion (see general comment (iii) and the new Fig. 14). This analysis just uses simply the mapping of ozone to PV and calculation of the respective gradient, as the PDF-related section should only be a side remark and not in the focus of the paper (see answer to the comment above).
As discussed already in our reply to the overall comment 2, there is agreement between MLS and CLaMS based gradients for parts of the season, but also some disagreement (not unexpected).

-p10606, L1-5: *The dynamical variability in the Arctic polar vortex and in the subtropical jet are also extremely large I would be astonished if that in the ASM circulation was larger than, for example, that during a strong SSW or a transient excursion of the subtropical jet around a strong ridge/trough pattern during both of which the transport barriers can nevertheless remain quite strong. It must be the *type* of dynamical variability rather than the magnitude that is critical?*

As discussed already above (see also reply to Reviewer 2), the new Fig. 14 and the discussion now relate the variability in the PV-gradient to convective activity, which seems to be the most important type of variability affecting the monsoon anticyclone (as found already by Randel et al., 2006).

-p10606, L12-15: *The ability to define a transport barrier over such a limited vertical range would seem, on the surface, to be a significant limitation of this method, which would be worth discussing a bit more. What do observations show with*

regard to the coherence of trace gas structures at levels above and below this? Over what vertical range do the dynamical fields e.g., the winds that define the anticyclonic circulation show a "closed" circulation? This is also another place where the question of the representativeness of 6 July 2011 is raised is that vertical structure consistent throughout the monsoon season, and in other years?

We discuss these issues now more extensively and critically at several places in the manuscript (e.g., Sect. 4, discussion).

-p10606, L21-23: *I dont understand this statement certainly crossing the tropopause is a sufficient condition for there to be a transport barrier but it is my no means a necessary condition.*

The sentence has been reworded.

-p10606, L24-25: *Surely there is no suggestion that a feature as large as the ASM boundary defined by the PV contours derived here could be considered "noise"?*

We removed this part of the sentence.

-p10607, L6-7: *Giving some indication (perhaps at least from the other two years that have been mentioned here) of the degree of interannual variability expected would be helpful.*

There is not much systematic difference evident from comparison of the three years 2011–2013, except a slightly broader distribution in longitude in 2012. This information has been added. Interannual variability of the anticyclone and related transport will be further studied in the future.

-p10607, L12: *It would be helpful to state what the longitudes of the Iranian and Tibetan Plateaus are.*

This information has been added.

-p10607, L15-21: *I dont understand the point that is intended here. Is this an argument for a physical basis for bimodality, or an argument that it is an artifact of the geometry?*

We think the bimodality in the longitudinal PV distribution is partly related to the projection and hence partly an artifact of the geometry. To what degree the bimodality in the longitudinal GPH maximum distribution has a physical basis needs to be further studied. We reworded the respective paragraph.

-p10607, L26-28: *It isnt clear to me from this statement how the change in extent/ location of the PV contours is related to the "conduit"?*

The sentence has been reworded.

-p10608, L1-8: *How would high-resolution (inherently highly localized in space and time) in situ observations help, when full spatial and temporal coverage of the region is needed to assess transport barriers and their variations? What is "sufficiently high resolution" (in the horizontal and vertical)? Here again, it would help to have given the vertical resolution of the model and of MLS, and to argue why these are or arent sufficient.*

The model and MLS resolutions are given now in Sect. 2. Indeed, a dense coverage of the monsoon region with high-resolution observations (vertical resolution at least similar to the model resolution, which is about 400 m) would be the best. However, to our knowledge such a dataset seems not available during the next years. But also in-situ measurements from aircraft flights could provide important information about the confinement of air (e.g., flights crossing the PV-gradient based barrier could be analysed for co-varying structure in trace gas mixing ratios). The whole paragraph has been reworded.

-p10608, L19: *See comment above re Nash et al.*

See our answer to the comment above.

WORDING AND FIGURE ISSUES, TYPOS:

-Figure 1: *The cyan line doesnt show up very well. What is the source of the data plotted in Figure 1?*

The source of the data plotted in Fig. 1 is ERA–Interim reanalysis, which is stated now explicitly in the figure caption.

-Figures 2, 9, 10, and 14 *(especially 9 and 10) are too small. I realize this is partly because of the limitations of the ACPD format, but it would be good to insure that they are larger in the final ACP version.*

This should indeed be due to the ACPD format. We will ensure that the figures appear larger in the final ACP version.

-Figure 2 caption, *second to last line, "is" should be "are"*

Corrected.

-The Figure 11 *color palette and symbols are difficult to read. The black symbols tend to disappear on the dark brown in the CO panel. I would suggest using a brighter color palette and/or a different symbol color perhaps even two different colors for the symbols for PV and CO gradients.*

We changed the symbols to improve the presentation quality (see also reply to Reviewer 2).

-p10594, L10: *replacde "notwithstanding" with "nevertheless"*

Done.

-p10596, L13: *"focusses" should be "focuses"*

Corrected.

-p10596, L15-16: *UTLS already defined on p10594*

We removed the definition here.

-p10597, L25: *in the parenthetical statement either commas or nested parentheses are needed*

Changed.

-p10598, L9: *Figures 2a and b show*

Corrected.

-p10598, L10; p10600, L13; p10603, L10: *The use of "exemplarily" here does not seem appropriate when what you mean is something like "as an example".*

We reworded both sentences avoiding "exemplarily" now.

-p10599, L1: *"to" should be "on"*

Corrected.

-p10599, L7: *"shedded" should be "shed"*

Corrected.

-p10599, L19: *add a comma after "structure"*

Done!

-p10600, L13: *Fig. 5 is introduced before Fig. 4 is discussed, thus it would make more sense to switch those figure numbers.*

Thanks for pointing this out! Because later parts of Sect. 4 correspond to Fig. 5, we would like to keep the order. Therefore, we briefly introduce Fig. 4 now at the beginning of the paragraph, before turning to Fig. 5.

-p10600, L14: *"mosoon" should be "monsoon"*

Corrected.

-p10601, L20-21: *Suggest changing "We apply an additional constraint to exclude the subtropical jet from the calculation, which generally shows much larger PV-gradient values" to "We apply an additional constraint to exclude from the calculation the subtropical jet, which generally shows much larger PV-gradient values"*

Changed as suggested.

-p10603, L24: *add a comma after "variability"*

Changed.

Manuscript prepared for Atmos. Chem. Phys.
with version 3.2 of the LaTeX class copernicus.cls.
Date: 14 August 2015

A PV-based determination of the transport barrier in the Asian summer monsoon anticyclone

F. Ploeger[1], C. Gottschling[1], S. Griessbach[1], J.-U. Grooß[1], G. Guenther[1], P. Konopka[1], R. Müller[1], M. Riese[1], F. Stroh[1], M. Tao[1], J. Ungermann[1], B. Vogel[1], and M. von Hobe[1]

[1]Institute for Energy and Climate research: Stratosphere (IEK–7), Forschungszentrum Jülich, Jülich, Germany.

Abstract. The Asian summer monsoon provides an important pathway of tropospheric source gases and pollution into the lower stratosphere. This transport is characterized by deep convection and steady upwelling, combined with confinement inside a large-scale anticyclonic circulation in the upper troposphere and lower stratosphere (UTLS). In this paper, we show that a barrier to horizontal transport along the 380 K isentrope in the monsoon anticyclone can be determined from a local maximum in the gradient of potential vorticity (PV), following methods developed for the polar vortex (e.g., Nash et al., 1996). Due to large dynamic variability of the anticyclone, this maximum in the PV gradient is weak and additional constraints are needed (e.g., time averaging). Nevertheless, PV contours in the monsoon anticyclone agree well with contours of trace gas mixing ratios (CO, O_3) and mean age from model simulations with a Lagrangian chemistry transport model (CLaMS) and satellite observations from the Microwave Limb Sounder (MLS) instrument. Hence, the PV-based transport barrier reflects the separation between air inside the anticyclone core and the background atmosphere well. For the summer season 2011 we find an average PV value of 3.6 PVU for the transport barrier in the anticyclone on the 380 K isentrope.

1 Introduction

An efficient pathway for anthropogenic pollution and tropospheric source gases into the stratosphere is linked to the Asian summer monsoon, as has been shown from satellite observations of HCN (Randel et al., 2010). Upward transport in the monsoon is caused by frequent high-reaching convection (e.g., Tzella and Legras, 2011; Bergman et al., 2012) and slower steady upwelling at higher levels around the tropopause. In the upper troposphere and lower stratosphere (UTLS), more precisely in the Tropical Tropopause Layer TTL (e.g., Fueglistaler et al., 2009), the Asian monsoon is characterized by a large-scale anticyclonic circulation system, mainly a response to strong convective diabatic heating at low levels (Gill, 1980). The anticyclonic circulation confines the upward transported air and isolates it, to some degree, from its surroundings. This confinement leads to positive anomalies of tropospheric trace gases (e.g., CO, HCN, H_2O) and to negative anomalies of stratospheric trace gases (e.g., ozone) in the anticyclone (e.g., Randel and Park, 2006; Park et al., 2007, 2008; James et al., 2008; Bian et al., 2012).

For an improved understanding of the pollution transport by the monsoon, understanding the confinement of trace gases within the anticyclone is crucial. However, the Asian monsoon anticyclone is characterized by large dynamic variability (Garny and Randel, 2013), strong east-west displacements (Krishnamurti et al., 1973), frequent shedding of small-scale eddies (Hsu and Plumb, 2000; Popovich and Plumb, 2001) and even splits. Moreover, strong diabatic heating processes play a role in the monsoon and, consequently, PV is not well conserved (e.g., Holton, 1992). For these reasons, the confinement of air inside the Asian monsoon anticyclone appears much weaker than in the polar vortex, and it turns out to be very challenging to locate a barrier to horizontal transport (Garny and Randel, 2013). However, that such a transport barrier exists, at least to some degree, is reflected in the observed trace gas anomalies within the anticyclone. To date, simplified criteria have been adopted to define this transport barrier and to separate the core region of the anticyclone from its surroundings. These criteria are commonly based on the positive geopotential height (GPH) anomaly or the negative PV anomaly in the monsoon anticyclone and assume a fixed GPH (on a fixed pressure level) or PV value to represent the transport barrier (e.g., Randel and Park, 2006; Bergman et al., 2013). These criteria have the advantage of being easy to apply, but they lack a clear

Correspondence to: F. Ploeger (f.ploeger@fz-juelich.de)

physical reasoning.

In this paper, we present a physically motivated criterion to deduce the transport barrier in the Asian monsoon anticyclone based on conservation properties of the flow. This criterion is closely related to a well-established methodology using PV gradients on isentropic surfaces, which has been originally developed for the polar vortex (e.g., Butchart and Remsberg, 1986; Manney et al., 1994; Nash et al., 1996). The method relies on the fact that PV is approximately conserved, such that a maximum in the PV gradient on an isentrope reflects the existence of a barrier to transport. We emphasize already here that the terminology "transport barrier" does not imply vanishing cross-transport. In fact, the anticyclone transport barrier turns out to be rather leaky and is better interpreted as a region of reduced cross-transport (see Sect. 7).

We introduce the data, model and methods used in Sect. 2. In Sect. 3 we motivate the use of PV as a basis for deducing the anticyclone transport barrier, by comparing PV to simulated and observed trace gas distributions (CO, O_3) in the Asian monsoon region. The criterion for deducing the transport barrier is presented in Sect. 4, and validated by comparison to simulated CO, ozone and mean age in Sect. 5. We finally discuss our results and conclude.

2 Methods

Meteorological fields to characterize the Asian monsoon anticyclone are taken from European Centre for Medium-Range Weather Forecasts (ECMWF) ERA-Interim reanalysis. ERA-Interim covers the period from 1979 until present, assimilating observational data from several sources to provide a reliable state of the atmosphere (for details, see Dee et al., 2011). We used 6-hourly data on a $1^\circ \times 1^\circ$ horizontal grid and interpolated it on potential temperature (θ) levels in the vertical. The presented analysis focuses on the summer season (June–August, JJA) 2011 and on the 380 K isentropic surface, which is a characteristic level for the Asian upper-level anticyclone in the UTLS. Note that in the tropics 380 K is close to the 100 hPa isobaric surface, which has been used in several studies to analyse transport in the Asian monsoon anticyclone (e.g., Randel and Park, 2006; Bergman et al., 2013).

The most relevant meteorological fields for this study are Ertel's potential vorticity (PV), the circulation (Γ), and the Montgomery stream function (M). PV is calculated from the horizontal winds (e.g., Holton, 1992)

$$\mathrm{PV} = \sigma^{-1}(\zeta + f), \qquad (1)$$

with ζ the relative vorticity, $f = 2\Omega\sin\phi$ the Coriolis parameter, and $\sigma = -g^{-1}\partial_\theta p$ the isentropic mass density (p pressure, ϕ latitude, g acceleration due to gravity). PV is a particularly well suited quantity for characterizing barriers to transport. In the absence of friction and diabatic processes

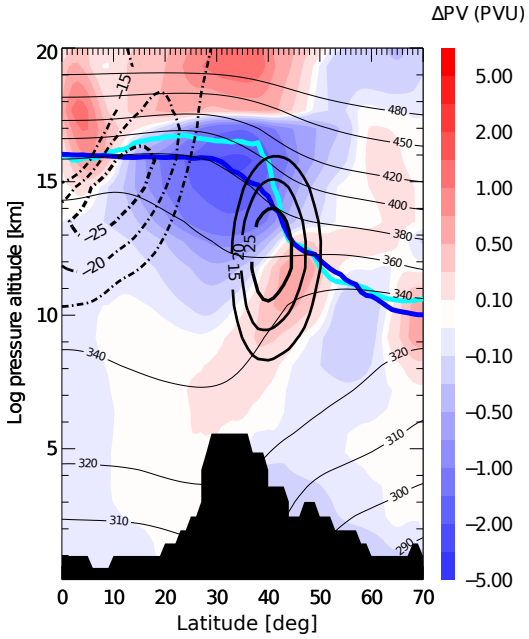

Fig. 1. Meteorological conditions in the Asian monsoon anticyclone (based on ERA–Interim reanalysis). Color shading shows the PV anomaly of the monsoon longitude section (60°-120°E) with respect to the zonal mean, averaged over summer (June-August). Also shown is zonal wind (thick black, solid/dashed positive/negative) and potential temperature (thin black) averaged between 60°-120°E. The first thermal tropopause (calculated using the definition of WMO, 1957) zonally averaged over 0°-360°E is shown as dark-blue, averaged over 60°-120°E as cyan line.

the PV of an air parcel is conserved following its motion (e.g., Holton, 1992), and thus regions of enhanced PV gradients are indicative of suppressed transport (transport barriers). This fact was used for the polar vortex to deduce the transport barrier based on the gradient of PV along an isentropic surface (e.g., Manney et al., 1994; Nash et al., 1996).

A related quantity, characterizing fluid rotation, is the circulation Γ along a closed contour S (here, on an isentrope)

$$\Gamma = \oint_S \mathrm{d}s \cdot \mathrm{v} = \int_A \mathrm{d}a\, \zeta, \qquad (2)$$

with A the area enclosed by the contour S and $\mathrm{v} = (u,v)$ the horizontal wind on an isentropic surface (ds and da represent line and area elements). Therefore, cyclonic flow is characterized by positive circulation, while anticyclonic flow is characterized by negative circulation.

The Montgomery stream function $\mathrm{M} = c_p T + \Phi$ (with Φ geopotential, T temperature, and c_p the specific heat at constant pressure) is the isentropic analogue of geopotential, which is frequently used to characterize the monsoon anticyclone (Randel and Park, 2006; Bergman et al., 2013). Under geostrophic approximations the horizontal flow on an isentrope is along contours of constant M (e.g., Holton, 1992).

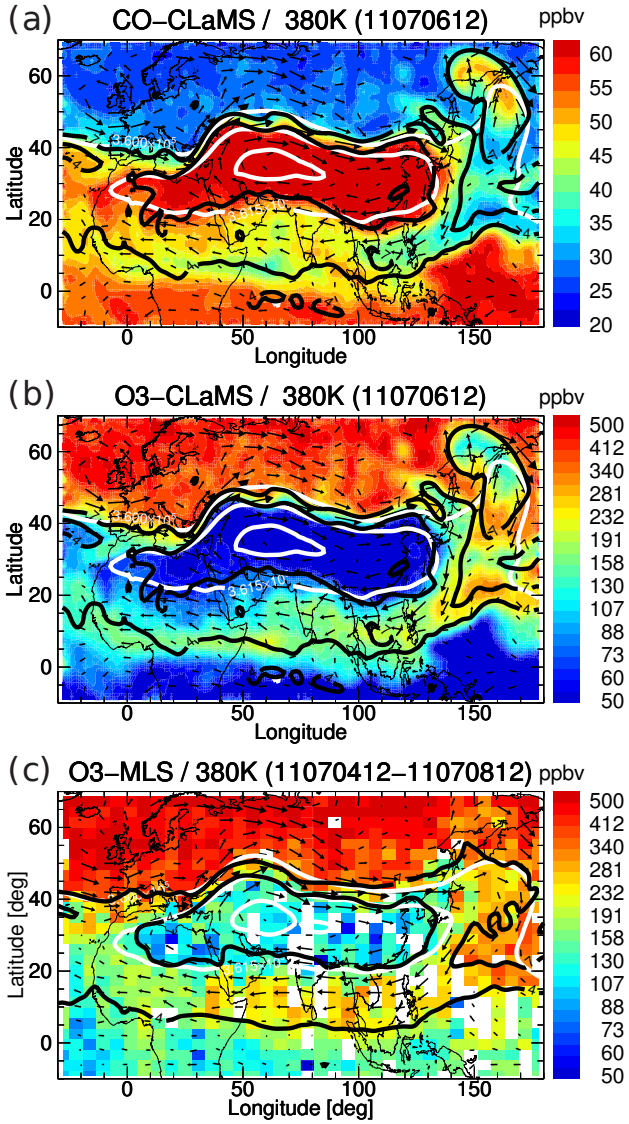

Fig. 2. Maps of (a) CLaMS CO and (b) CLaMS ozone on the 380 K isentrope on 6 July 2011 within the Asian monsoon region. Selected potential vorticity contours are shown in black (4, 7 PVU) and Montgomery stream function contours in white ($3.6 \cdot 10^5, 3.615 \cdot 10^5$ m^2/s^2). Arrows show horizontal wind. (c) Same but for MLS ozone during the period 4–8 July 2011, with the MLS data binned into $3^\circ \times 6^\circ$ latitude/longitude bins (bins without measurements are left white). Meteorological data are taken from ERA-Interim. (Note the logarithmic color scale for ozone.)

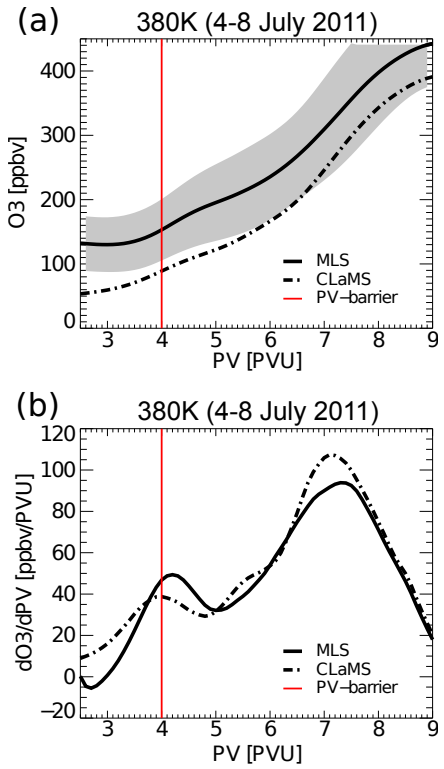

Fig. 3. (a) Ozone from MLS (solid) and CLaMS (dashed) versus potential vorticity in the Asian monsoon region (10°N-60°N and 10°W-160°E) at 380 K, averaged over the period 4-8 June 2011. (b) Same but for the ozone gradient with respect to potential vorticity. Red lines show the transport barrier determined from PV (see text).

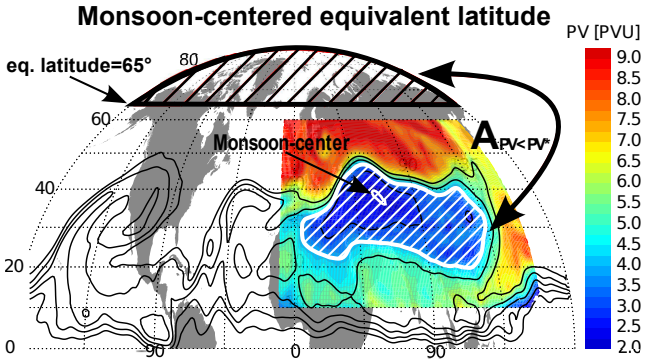

Fig. 4. Illustration of the calculation of monsoon-centered equivalent latitude from the area within PV-contours (see text for details). Color-coded is the PV-field within the Asian monsoon region at 380 K (10°N–60°N and 10°W–160°E) averaged for 5–7 July 2011, with the white contour highlighting 4 PVU. The black contours show PV globally.

Due to the anticyclonic nature of the upper-level circulation, the Asian monsoon in the UTLS is characterized by strongly negative, anomalously low PV (see Fig. 1), and anomalously high Montgomery stream function values. To

the north, the anticyclone is bounded by the subtropical westerly jet, to the south by the equatorial easterly jet. Furthermore, the monsoon region is characterized by an elevated thermal tropopause which, from a climatological point of view, exceeds the zonal mean tropopause by more than 1 km (Fig. 1), corresponding to $\approx$ 20K in potential temperature.

To confirm the deduced location of the transport barrier, which will be based on PV, we consider different trace gas species (carbon monoxide, ozone) from model simulations with the Chemical Lagrangian Model of the Stratosphere CLaMS (McKenna et al., 2002b,a; Konopka et al., 2007), driven by ERA-Interim meteorological data. We further consider simulated mean age of air, the average transit time for transport from the tropical tropopause, calculated from an inert tracer with a linearly increasing source in the model (e.g., Waugh and Hall, 2002). CLaMS is a Lagrangian chemistry transport model (CTM), based on 3D forward trajectories, with an additional parameterization for small-scale mixing, which depends on the deformation in the large-scale flow. Vertical transport in the model is purely diabatic above about 300 hPa, with the total diabatic heating rates taken from ERA-Interim forecast data. The vertical model resolution around the tropopause is about 400 m. For the simulation of CO, a lower boundary condition from MOPITT (Measurements of Pollution in the Troposphere satellite experiment) is used and chemical loss due to reaction with OH is included as described in Pommrich et al. (2014). CLaMS ozone includes a zero mixing ratio lower boundary condition and a simplified chemistry comprising photolytical production and loss due to reaction with OH. For further details about this specific CLaMS simulation see Pommrich et al. (2014). In the UTLS, CLaMS CO and ozone agree well with various observations, as shown in several recent publications (e.g., Pommrich et al., 2014; Konopka et al., 2010).

In addition, results will be compared to ozone observations from the Microwave Limb Sounder (MLS) instrument onboard the Aura satellite (Livesey et al., 2008). MLS scans about 3500 profiles per day providing a dense sampling of the global atmosphere, including the Asian monsoon region. The vertical resolution of MLS ozone is about 3 km. For MLS CO, a standard tropospheric tracer for Asian monsoon studies, the vertical resolution is coarser ($\approx$ 4.5 km) and therefore we focus on ozone for this study. MLS profiles are originally on pressure levels and were interpolated to potential temperature surfaces for the purpose of this study. For further details about MLS data, see Livesey et al. (2008).

3 Trace gas confinement in the anticyclone and PV

Figure 2a/b show the distributions of CLaMS CO and ozone in the monsoon region on the 380 K isentrope on 6 July 2011. Clearly visible is the positive anomaly of the tropospheric tracer CO and the negative anomaly of the stratospheric tracer ozone in the monsoon anticyclone, characteristic for strong tropospheric impact and confinement within the anticyclone. Note that extratropical stratospheric air is advected around the eastern flank of the anticyclone, transporting CO-poor and ozone-rich air equatorwards. This transport has recently been shown to strongly affect the ozone seasonality in the tropics (Konopka et al., 2010; Ploeger et al., 2012; Abalos et al., 2013). Furthermore, poleward transport of CO-rich air affects the trace gas composition of the lowermost stratosphere and crucially depends on the CO lifetime (e.g., Hoor et al., 2010). To create a similar map from ozone measurements, we bin ozone observations from MLS between 4 and 8 July 2011 (using version 3.3 data), in order to obtain sufficiently dense observations (Fig. 2c). Lower ozone mixing ratios in the model compared to MLS are likely related to the broad satellite averaging kernel and the zero mixing ratio lower boundary condition at the surface in the model (Pommrich et al., 2014). However, the patterns of the low ozone anomaly in the monsoon anticyclone reliably agree between model simulations and observations (note also the five-day average for the satellite data).

Overlaid on the trace gas mixing ratios in Fig. 2 are contours of PV and Montgomery stream function. Both meteorological quantities show strong anomalies within the monsoon. However, when compared to the trace gas mixing ratio contours the PV contours agree better than the Montgomery stream function contours, in particular for small-scale variations. Even the separation of a smaller eddy to the east of the main anticyclone is well reflected in the PV distribution. These small scale eddies, frequently shed from the main anticyclone, have the potential to transport air masses with elevated mixing ratios of tropospheric trace gases (e.g., CO, H_2O) rapidly into the middle and high latitude lower stratosphere (e.g., Ploeger et al., 2013; Vogel et al., 2014). A close relation between the distributions of CO and PV in the monsoon was already found by Garny and Randel (2013). For these reasons, we use PV as a basis for defining a criterion for the transport barrier in the Asian monsoon.

Motivated by studies of the polar vortex where the transport barrier is characterized by particularly steep gradients of conserved tracers, we map MLS and CLaMS ozone versus potential vorticity (Fig. 3). This mapping was carried out by binning all data from the Asian monsoon region at 380 K (10°N-60°N and 10°W-160°E) with respect to potential vorticity (bin size 0.1 PVU). Figure 3 shows that, despite the offset between CLaMS and MLS ozone mentioned above, there is agreement in the main structure, with low ozone in the core of the anticyclone (at low PV values) and higher mixing ratios towards higher PV. In particular, there is evidence from model and observations for a two-step increase of ozone mixing ratios, resulting in two separate maxima in the gradient of ozone with respect to PV. The stronger maximum around 7 PVU is related to the transport barrier at the subtropical jet (Kunz et al., 2011). The secondary maximum occurs around 4 PVU. In the following, we will provide evidence that this secondary maximum may be interpreted as the transport bar-

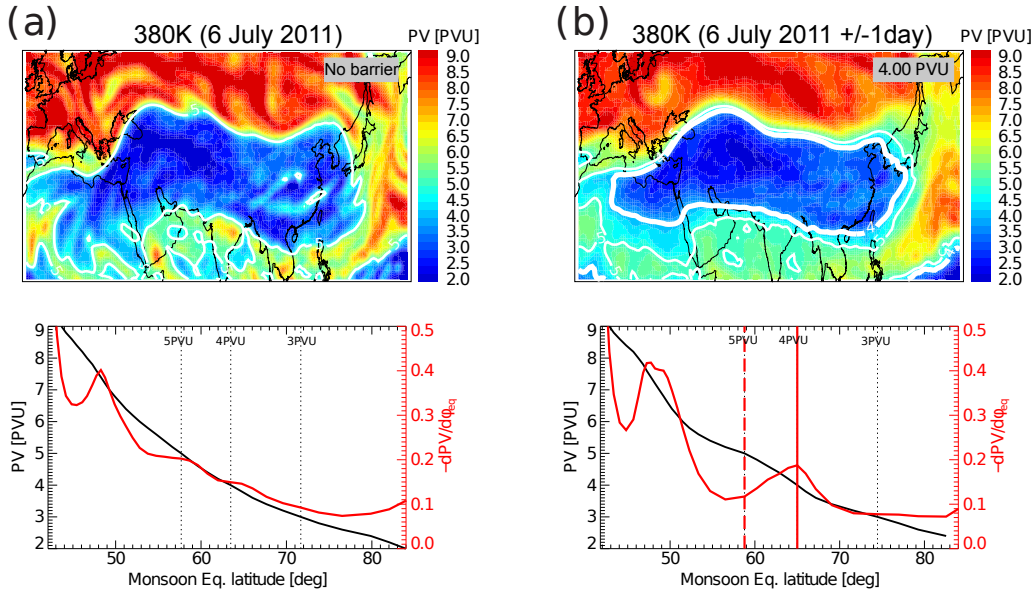

Fig. 5. (a) Potential vorticity map at 380 K on 6 July 2011, in the Asian monsoon region between 10°-60°N and 10°W-160°E (upper panel), and PV as function of the monsoon centered equivalent latitude (lower panel). Monsoon equivalent latitude ϕ_{eq} is calculated from the area within PV contours (see text). Shown is PV(ϕ_{eq}) (black) together with the respective PV gradient $\partial PV/\partial\phi_{eq}$ (red). Low PV and large ϕ_{eq} indicate the anticyclone center. (b) Same as (a) but for the PV-field averaged between 5 and 7 July 2011. The anticyclone transport barrier, deduced from a local maximum in the PV gradient (see text), is shown as white thick contours (upper panels) and red solid vertical lines (lower panels), respectively. White thin contours (upper panels) and red dashed lines (lower panels) show 5 PVU. Black dashed lines (lower panels) highlight particular PV values. The PV-value of the barrier is given in the grey box.

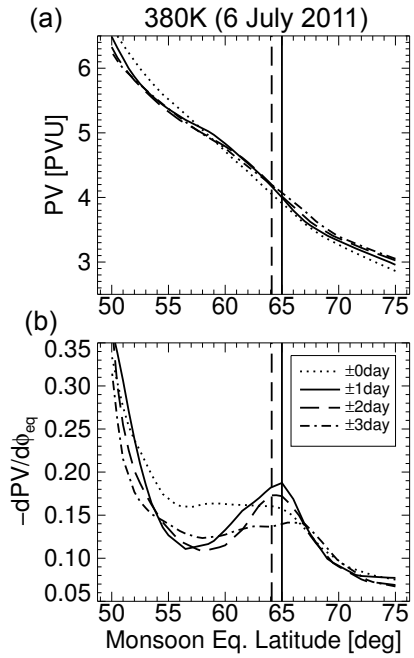

Fig. 6. (a) Potential vorticity with respect to monsoon centered equivalent latitude on the 380 K isentrope, with the PV field averaged over different periods centered around 6 July 2011. (b) The corresponding gradients of PV with respect to equivalent latitude. Vertical lines show the PV-gradient maximum.

rier of the Asian monsoon anticyclone (red line shows the transport barrier PV value, objectively determined using the criterion derived in the following section).

4 A PV-gradient criterion for the Asian monsoon

Motivated by the good agreement between the PV and trace gas varability in the monsoon region (Fig. 2) and the fact that PV is an approximately conserved quantity, we follow the approach developed for the polar vortex for deducing a transport barrier (e.g., Butchart and Remsberg, 1986; Manney et al., 1994; Nash et al., 1996). Nash et al. (1996) defined the transport barrier of the vortex edge as the location of the largest (isentropic) change in PV, with the additional constraint of close proximity to a strong zonal jet. Recently, Kunz et al. (2011) deduced the location of the transport barrier for the subtropical jet using an analogous approach.

The PV distribution on 6 July 2011 is shown in Fig. 4, illustrating the anomalously low PV in the Asian monsoon anticyclone. In a first step, we restrict all fields to a region including the monsoon anticyclone, which we define as $10°N \leq \phi \leq 60°N$ and $10°W \leq \lambda \leq 160°E$ (ϕ latitude, λ longitude) to eliminate the interfering influence of low PV values near the equator. The PV distribution on 6 July 2011 within this region is shown in Fig. 5a (top). A similar definition of the Asian monsoon area was used by Garny and

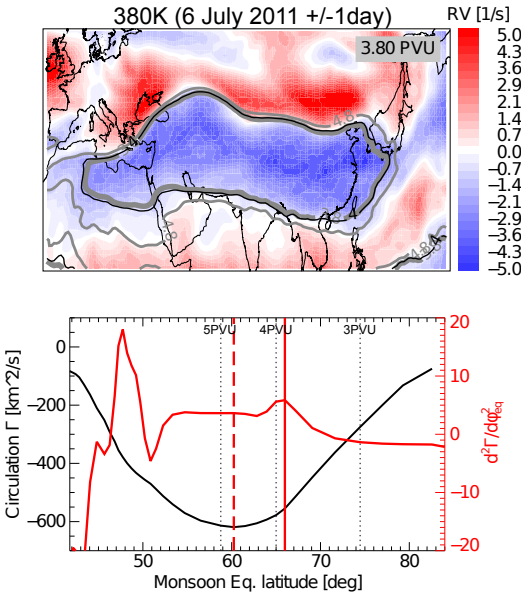

Fig. 7. Relative vorticity map at 380 K, in the Asian monsoon region between 10°-60°N and 10°W–160°E averaged over 5-7 July 2011 (upper panel). The lower panel shows the horizontal circulation (calculated from area-integrated relative vorticity) as function of the monsoon centered equivalent latitude (black) and the respective second derivative (red). PV-values corresponding to the minimum circulation are shown as thin grey contour (upper panel) and red dashed line (lower), and PV-values corresponding to the maximum in the second derivative of the circulation as thick grey contour (upper) and red solid line (lower). The black contour (upper panel) shows the transport barrier PV deduced from the maximum PV-gradient, for comparison. (See text for further details).

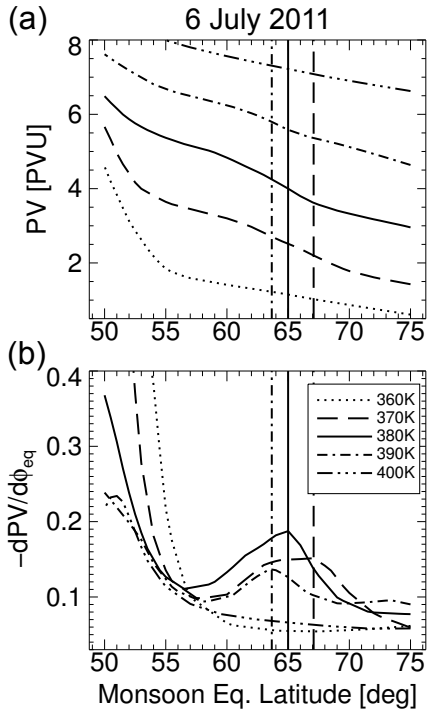

Fig. 8. (a) Potential vorticity with respect to monsoon centered equivalent latitude on 6 July 2011, on different levels (360 K, 370 K, 380 K, 390 K, 400 K isentropes). (b) The corresponding PV-gradients with respect to equivalent latitude. Vertical lines show the gradient maxima (transport barriers).

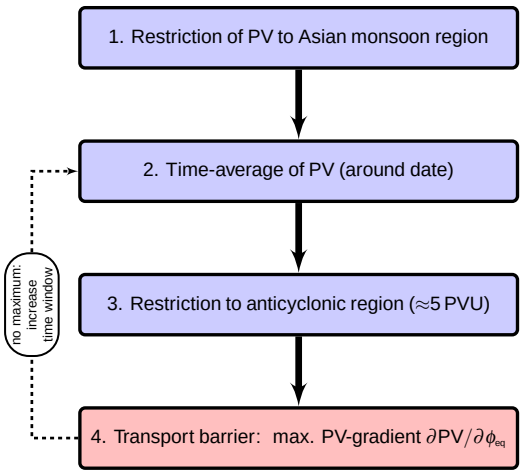

Fig. 9. Method to localize the PV-based transport barrier in the Asian monsoon anticyclone (at 380 K), summarized in four steps.

Randel (2013). The chosen latitude/longitude range includes the anticyclone for all days during summer 2011. Slight variations to this range cause no significant change to our results.

Following Butchart and Remsberg (1986), we define a monsoon-centered equivalent latitude ϕ_{eq} of a given PV contour in the anticyclone as the latitude of a circle around the North pole enclosing the same area, as illustrated in Fig. 4 (here, the 4 PVU contour is mapped to $\phi_{eq} = 65°$). Hence, for a PV contour enclosing an area A, the equivalent latitude is defined by $A = 2\pi r_E^2 (1 - \sin\phi_{eq})$, with r_E the Earth's radius. Consequently, the center of the monsoon occurs at a monsoon equivalent latitude of 90°, corresponding to the location of minimum PV. In this sense, PV and equivalent latitude are related to each other, exhibiting a unique functional dependence PV(ϕ_{eq}) as shown in Fig. 5a (bottom). As already noted above, PV increases monotonically from low values in the center of the anticyclone to higher values at its edge.

For 6 July 2011, the gradient of PV with respect to ϕ_{eq}, namely $\partial PV/\partial\phi_{eq}$, shows no clear maximum indicative for the anticyclone transport barrier, besides the maximum around 50° equivalent latitude (about 7–8 PVU) related to the transport barrier of the subtropical jet (Kunz et al., 2011). The absence of a clear secondary maximum, representing the anticyclone transport barrier, has recently been attributed to the large dynamical variability of the anticyclone (Garny and Randel, 2013). However, if this variability is damped by averaging the PV field over a time window of 3 days between 5

and 7 July 2011, a clear secondary maximum in the PV gradient emerges around 65° equivalent latitude (Fig. 5b, bottom). In the following, we interprete this maximum as the transport barrier of the Asian monsoon anticyclone, and show its physical significance by comparison to trace gas distributions in Sect. 5.

To calculate the time averaged PV for different dates we use a variable time window. Therefore, we define an optimal window for each date as the smallest number of days (±3 days at most) such that the PV-gradient maximum exceeds the adjacent minima by 30%. Figure 6 illustrates this procedure for the example of the 6 July 2011, confirming that for this date a ±1 day average (3-day time window) results in the clearest gradient maximum. If the time window is chosen too large (e.g., ±3 days in Fig. 6), the maximum in the PV gradient degrades again because different dynamical conditions contribute to the average. For that reason, we average maximum over 7 days (given date ±3 days). Notably, for some dates no time averaging is necessary to determine a PV-gradient maximum.

We apply an additional constraint to exclude from the calculation the subtropical jet, which generally shows much larger PV-gradient values than the anticyclone transport barrier. Empirically, for the summer 2011 a PV-limit of 5 PVU reliably separates the monsoon transport barrier from the subtropical jet at 380 K, as illustrated in Fig. 5b for July 6. A physical motivation for this constraint can be deduced from the horizontal circulation (also averaged over ±1 day, see Fig. 7), as described in the following. Necessarily, the anticyclone transport barrier is located within the region of anticyclonic motion (negative relative vorticity), and hence in the equivalent latitude range where the circulation decreases when moving away from the anticyclone center (hence, with decreasing monsoon equivalent latitude). Consequently, the PV-gradient maximum of the anticyclone transport barrier needs to be located at equivalent latitudes lower than the minimum circulation (4.8 PVU in Fig. 7). This circulation constraint generally excludes the subtropical jet from the transport barrier calculation. For simplicity, we use 5 PVU as an upper PV-limit for the transport barrier calculation at 380 K in the following, which is a good approximation of the circulation minimum. Note in addition that the second derivative of the circulation with respect to equivalent latitude $\partial^2\Gamma/\partial{\phi_{eq}}^2$ is related to the first derivative of PV (see Eq. 2). Therefore, the transport barrier related to the local maximum in the PV gradient can be approximated by the local maximum in the second derivative of Γ (see Fig. 7, bottom), providing a consistency check of our procedure.

A necessary condition for the transport barrier criterion to hold is the existence of a strong PV-anomaly. Therefore, the applicability is restricted to a shallow layer around 380 K (see Fig. 1). Figure 8 compares PV and its gradient with respect to monsoon equivalent latitude at different levels for 6 July 2011. The PV-gradient based transport barrier turns out to be clearest at the 380 K level, still detectable at 370 K and 390 K, but becomes undetectable below (360 K) and above (400 K). Strongest PV-gradients at 380 K emerge not only for the 6 July, but during the whole summer (not shown). Note that the corresponding PV-values change between different levels, due to the strong dependence of PV on altitude. At levels of the subtropical jet core around 360 K, the strong jet to the north of the monsoon masks the existence of the anticyclone transport barrier (Garny and Randel, 2013).

The tropopause within the monsoon is located at particularly high altitudes (see Fig. 1). Compared to the zonal mean, the tropopause is upward bulging in the monsoon anticyclone by about 20 K potential temperature (Fig. 1). Therefore, the detectable PV-gradient based transport barrier around 380 K could likely be related to the tropopause, with air inside the anticyclone being tropospheric and surrounding air stratospheric. Consequently, the diagnosed transport barrier can also be interpreted as a PV-based tropopause definition, separating tropospheric and stratospheric air masses inside and outside of the anticyclone. Although enhanced PV gradients as a measure for confinement of air are detectable only within a shallow layer around the tropopause, the transport processes in the Asian monsoon occur throughout a thick layer from the surface to the lower stratosphere. As pointed out by Randel and Park (2006), the anticyclone at upper levels is strongly related to convective variability below.

To summarize, the minimum circulation (approximately 5 PVU) defines the *anticyclone boundary*. The *anticyclone transport barrier* is then calculated from the time-averaged PV field as the maximum PV gradient at PV values smaller than 5 PVU. The procedure is illustrated in Fig. 9, and generally results in a well defined PV-value (e.g., 4 PVU for 6 July 2011, see Fig. 5b) characterizing the transport barrier for the Asian monsoon anticyclone for most days between about mid June and mid August 2011. For some days during the summer season, however, no clear maximum emerges in the PV-gradient even after averaging over a few days (see also Fig. 12), possibly related to enhanced convective activity of the anticyclone during these days (see Fig. 12, and compare also Garny and Randel, 2013).

5 PV-based transport barrier and relation to trace gases

To investigate whether the diagnosed transport barrier is physically meaningful, in the sense of separating air masses of different chemical characteristics, we compare it to simulated CO in the Asian monsoon region. Figure 10 shows PV and CO maps at 380 K for the 6, 9, 12, 15, 18 and 21 July 2011, overlaid with the PV contours of the transport barrier (thick white), as deduced for each date following the procedure described in Sect. 4. First, the barrier calculated from the time averaged fields results in reasonable PV values also when compared to the instantaneous PV maps on the particular days. Second, in the CO distributions the diagnosed

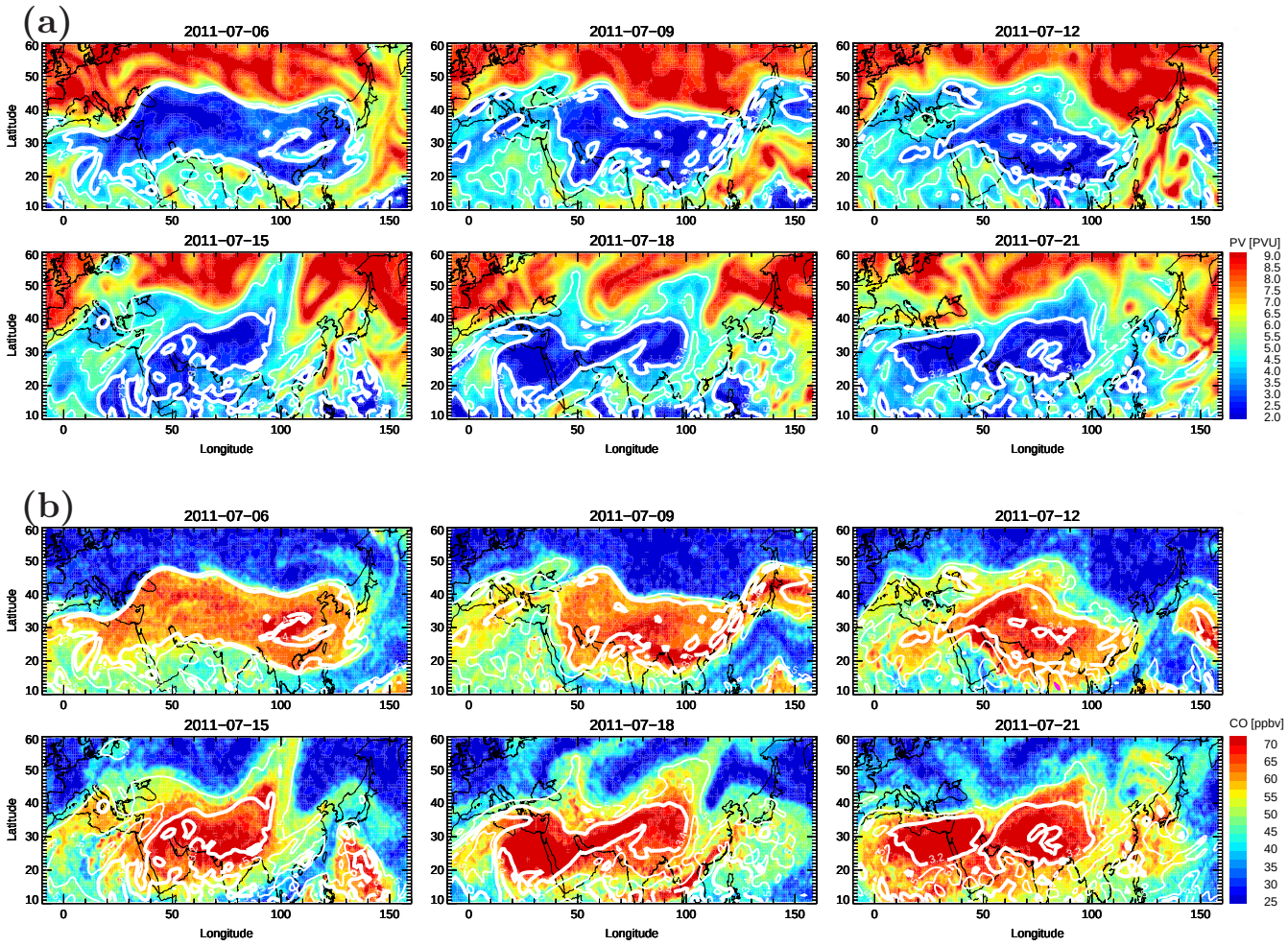

Fig. 10. (a) Potential vorticity maps at 380 K on 6/9/12/15/18/21 July 2011. The thick white contour shows the calculated anticyclone transport barrier (maximum PV gradient), the thin white contour 5 PVU. (b) Maps of CO from CLaMS on the same days, with PV-based transport barrier included as white contours.

barrier separates the high mixing ratios in the center of the anticyclone from the lower values around.

The sequence of plots in Fig. 10 illustrates the large variability of the anticyclone, with frequent shedding of smaller scale eddies (9 July) and even splits of the anticyclone (21 July). Also for days of particularly large variability the diagnosed barrier separates the core region of the anticyclone, characterized by high CO mixing ratios, well from its surroundings. Even the shedding of the smaller eddy and the vortex split are reflected in the transport barrier. It should be further noted that the agreement between PV and CO is not perfect and that high CO mixing ratios may extend outside the PV contour (e.g., on 17 July at the northeastern edge of the anticyclone), a potential indication for the leakiness of the anticyclone transport barrier.

To investigate more quantitatively to what degree the transport barrier deduced from PV is reflected in the CO distribution, we apply the barrier calculation to CO, exemplarily for 6 July 2011. Therefore, we restrict the CO field to the monsoon region, average over ± 1 days (5-7 July 2011), transform to PV-based monsoon centered equivalent latitude ϕ_{eq}, restrict to the anticyclonic region and calculate the PV-value of the maximum CO gradient $\partial \mathrm{CO}/\partial \phi_{eq}$. Figure 11a shows that a clear CO-gradient maximum emerges around 65°, equivalent to a PV value of 4 PVU, in agreement with the transport barrier deduced from the maximum PV-gradient. Likewise, distributions of simulated ozone and mean age of air reflect the PV-based transport barrier within the Asian monsoon region (Fig. 11b/c).

The PV-gradient based transport barrier for the Asian monsoon anticyclone has been calculated for all days between 20 June and 20 August 2011. Before this period and afterwards, almost no barrier could be found. CLaMS CO fields show trace gas confinement inside the anticyclone from mid of June 2011 onwards, but obviously the transport barrier during this early phase is not strong enough to

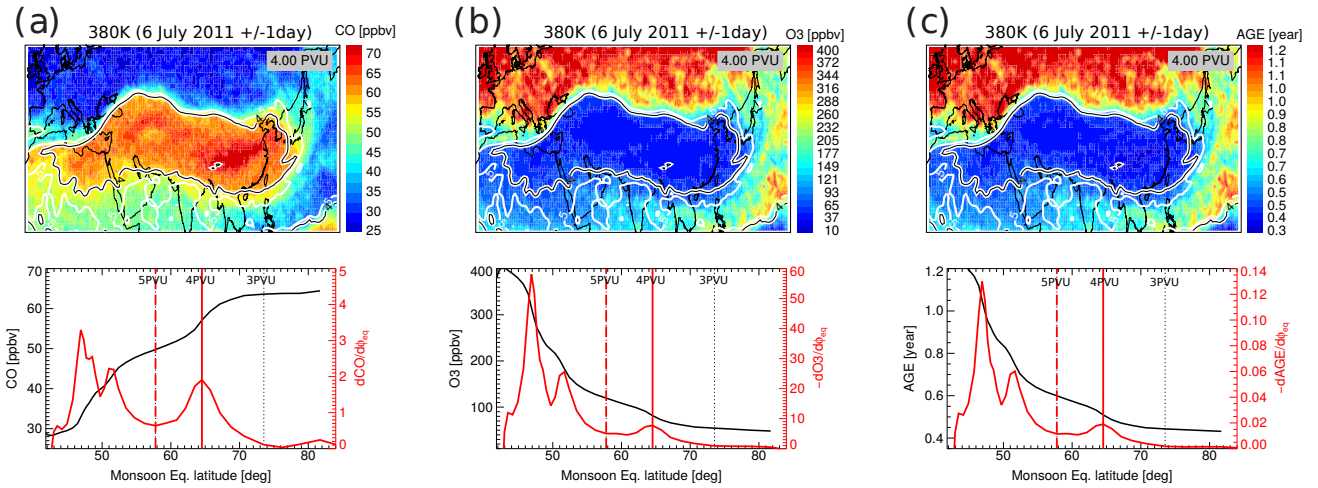

Fig. 11. (a) Map of CO from CLaMS on the 380 K isentrope, with the thick white contour showing the PV-value of maximum CO-gradient, the black contour showing the PV-value of maximum PV-gradient (thin white line shows 5 PVU), averaged between 5 and 7 July 2011 at 380 K. The bottom panel shows CO from CLaMS versus monsoon centered equivalent latitude (black), and the respective gradient (red). (b) Same for ozone from CLaMS, and (c) for mean age from CLaMS. (The PV values of the maximum gradient are given in the upper panels.)

be detectable by our method. Likewise, following the main monsoon season first the PV-gradient maximum vanishes (by mid–end of August) but trace gas anomalies remain for a few weeks until mid September. Hence, only during the main monsoon season the degree of confinement inside the anticyclone is strong enough for a PV-gradient maximum to be deducable.

Figure 12 (top) shows the evolution of the PV-gradient at 380 K over the summer season. Although the gradient maximum related to the anticyclone barrier appears weaker during some periods, it shows smooth subseasonal variability, with higher PV values (around 4 PVU) at beginning of July and beginning of August and lower PV values (around 3.2 PVU) in mid July and mid August. Significant subseasonal dynamic variability of the Asian monsoon, occurring with a frequency of about 30 days, has been recently noted by Garny and Randel (2013). Only for a few days (end of June and beginning of August) no transport barrier could be deduced because no clear maximum in the PV gradient emerged.

The evolution of the gradients of CO, ozone and mean age over the summer (Fig. 12b–d) consistently show a local maximum throughout most of the season, well coinciding with the PV-based transport barrier. Only by the end of July and after August 15, there is additional structure in the trace gas distributions at PV values above 4 PVU, which is not reflected in the PV gradients. During these periods, the maximum trace gas gradients are located at higher PV values than the PV-based transport barrier. In particular at the end of July, this behaviour follows strong convective activity (around 15 July), as seen from minimum outgoing longwave radiation (OLR) and maximum vertically integrated total diabatic heating rate $d\theta/dt$ (Fig. 12e). Here, daily gridded OLR data from NOAA-CIRES (see http://www.esrl.noaa.gov/psd/data/ and Liebmann and Smith, 1996) were averaged over the monsoon region (15°N–30°N and 60°E–120°E, as used also by Randel and Park, 2006). The ERA–Interim heating rates (only positive values) were integrated over the vertical range 300–370 K and averaged over the same region to provide a reanalysis based proxy for large-scale convection. Both convective proxies show a correlation of $r = -0.62$. As discussed by Randel and Park (2006), diabatic heating related to strong convection affects the anticyclonic monsoon circulation and increases the area of low PV values. Visual inspection of Fig. 12 suggests that increases in the barrier PV-value during beginning of July, end of July and mid-end of August follow enhanced convective activity. How significantly convection impacts the strength of the transport barrier, and which other processes are involved, needs to be further studied.

At 380 K, the PV value at the determined transport barrier is generally found between about 3 and 4 PVU, and shows intraseasonal variability. The mean PV value of the transport barrier over the summer 2011 is 3.6 PVU (at 380 K), in very good agreement with the mean PV of the related CO-gradient maximum (Table 1). We calculated the transport barrier PV values also for summers 2012 and 2013 (see Table 1) and found some weak interannual variability which needs to be further investigated. Note that the interannual variability and model projected future changes of the Asian monsoon anticyclone are largely uncertain, hitherto (e.g., Kunze et al., 2010).

6 Anticyclone location probability

The location probability for the region enclosed by the transport barrier (“anticyclone core region”, in the following) is shown in Fig. 13. Presented is the local frequency of occur-

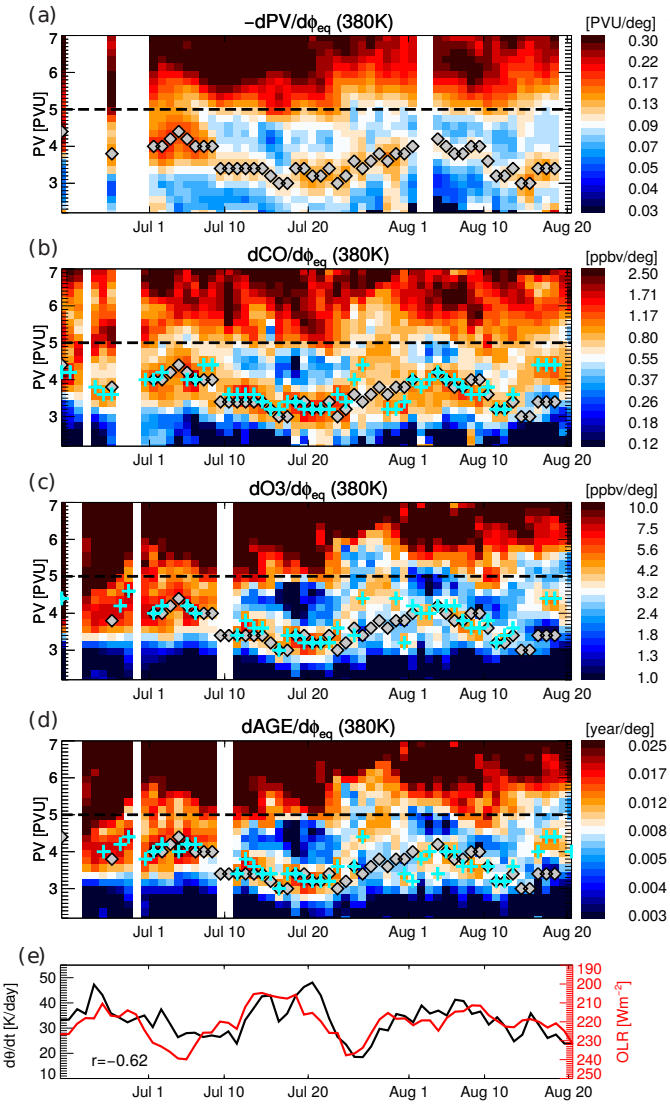

Fig. 12. (a) Time evolution of the gradient of PV with respect to monsoon centered equivalent latitude ϕ_{eq} as a function of PV for June-August 2011 at 380 K (note the logarithmic color scale). (b) Same but for CO. Symbols show the PV-gradient maximum (grey diamonds), and the CO-gradient maximum (green crosses). The dashed line highlights 5 PVU. Dates without a clear gradient maximum are left white. (c) Same but for O_3, and (d) for mean age. (e) Vertically integrated total diabatic heating rate from ERA-Interim (black) and outgoing longwave radiation (red), averaged over the monsoon region (see text for details). The correlation coefficient between the two quantities is given in the figure ($r = -0.62$).

Table 1. Transport barrier PV values for the Asian monsoon anticyclone at 380 K calculated from maximum PV and CO gradients and maximum-minimum ranges for the years 2011–2013 (averages over all dates between 20 June and 20 August of each year where the transport barrier criterion holds).

	2011	2012	2013
PV–barrier/PVU	3.6 (3.0–4.4)	3.8 (2.6–4.4)	3.5 (2.6–4.4)
CO–barrier/PVU	3.7 (3.2–4.4)	3.7 (2.4–4.6)	3.6 (2.6–4.2)

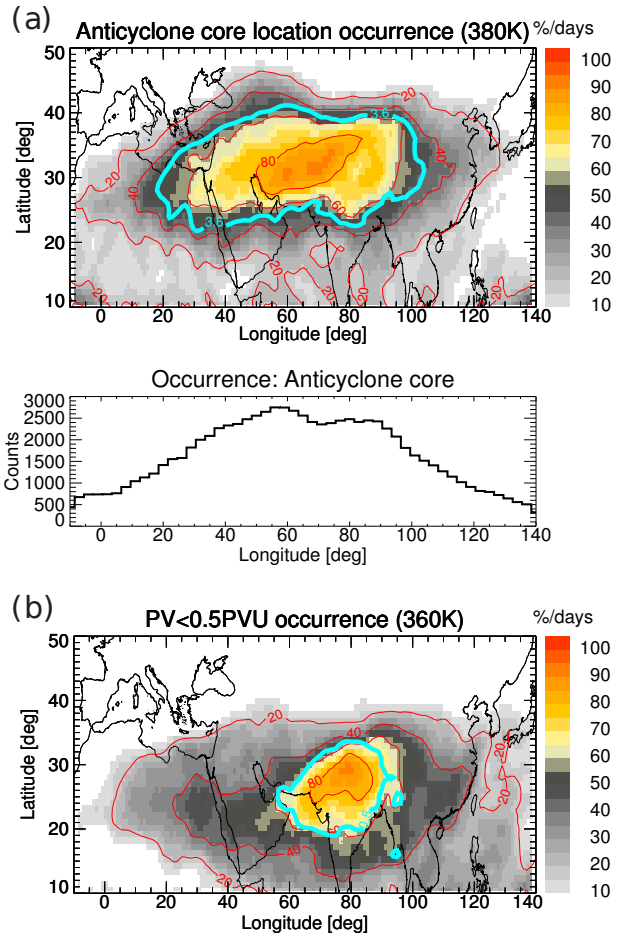

Fig. 13. (a) Occurrence frequency of the Asian monsoon anticyclone at 380 K (in percentage of days) for the period between 20 June and 20 August 2011, calculated from the area covered by PV values lower than the anticyclone transport barrier. Red contours show selected percentage values, the thick cyan contour shows the average PV value of the barrier in the average PV field (average over period considered). The bottom panel shows the projection of anticyclone occurrence frequency onto the longitude axis (bin size 2.5°). (b) Occurrence frequency for PV values below 0.5 PVU at 360 K isentrope, for the same period.

505

rence for PV values lower than the anticyclone barrier value, in units of percentage of days during summer 2011 (20 June to 20 August 2011). Clearly, the largest probability of being

located inside the anticyclone core occurs around 70°E/30°N (above 80% of the considered days). The whole region between about 25°–40°N and 20°–100°E is located within the anticyclone core for more than 50% of the days. Note that the anticyclone location probability may show significant inter-annual variability (e.g., a broader distribution in longitude in 2012 compared to 2011 and 2013) which needs to be further studied.

Zhang et al. (2002) and Yan et al. (2011) found an enhanced probability for the anticyclone center (estimated as geopotential height maximum) to occur at longitudes of the Tibetan (around 70–100°E) and the Iranian (around 45–65°E) plateaus, resulting in a bimodal longitude occurrence frequency. Figure 13a shows no enhanced probability for the anticyclone core region to be located in these two regions. Inspection of daily PV maps shows that the area of lowest PV rotates clock-wise with the anticyclonic flow (not shown). Similar to a children's roundabout such a rotation would cause no preferred locations for the anticyclone in the horizontal plane, if the rotation velocity was constant. However, if projected onto the longitude axis, the anticyclone location probability indicates two weak maxima (Fig. 13a/bottom), located at about 55°E and 85°E. Hence, it could be that the bimodality of the anticyclone longitude occurrence frequency is related, at least partly, to the projection of the (anticyclonic) rotation onto the longitude axis, and hence is an artifact of the projection. To what degree the bimodality in the longitudinal geopotential height maximum distribution, which is much clearer than for PV (see Zhang et al., 2002), has a physical basis and originates from enhanced occurrence probability in particular geographic regions needs to be further studied.

Note that the large zonal extent of the anticyclone occurrence probability at 380 K in Fig. 13a is related to frequent eddy shedding events, with the above analysis not distinguishing between the main anticyclone and westward and eastward travelling eddies. Further note that at lower levels (e.g., at 360 K in Fig. 13b) the region of lowest PV values is more confined and located further eastward and southward above the Tibetan plateau and Northern India, in the region of the vertical conduit for upward transport in the monsoon proposed by Bergman et al. (2013).

7 Discussion

Recently, Bergman et al. (2013) showed evidence for upward transport in the Asian monsoon occurring in a vertical conduit separated from the main anticyclone. Hence, it is not the anticyclone itself but this conduit which defines the most efficient pathway of polluted surface air to higher altitudes. However, as the air is released from the conduit at greater altitudes, it stays confined and chemically isolated, at least to some degree, inside the anticyclone, as shown from trace gas observations (e.g., Park et al., 2007, 2008). Therefore, a complete understanding of pollution transport from the boundary layer into the stratosphere requires understanding of the confinement inside the upper level anticyclone.

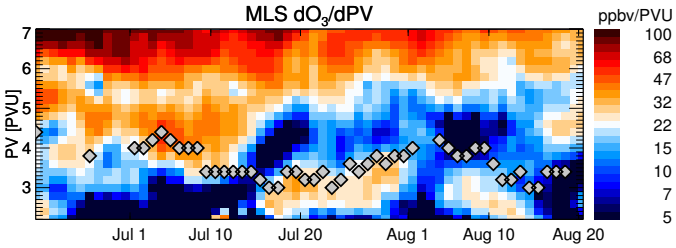

Fig. 14. Time evolution of the gradient of ozone from MLS with respect to PV (from ERA-Interim) for June-August 2011 at 380 K (note the logarithmic color scale). At each date, MLS measurements from 2 days before to 2 days later have been collected, to yield a sufficient coverage of the monsoon region. Grey symbols show the PV-gradient maximum.

In this paper, we investigated to what extent meteorological fields and trace gas distributions reflect the existence of a barrier to (quasi-) horizontal transport along isentropic surfaces in the Asian monsoon anticyclone. We refined the methodology developed for the polar vortex by additional constraints (e.g., time averaging, restriction to anticyclone) and found a secondary maximum besides the subtropical jet maximum in the gradient of potential vorticity with respect to a monsoon centered equivalent latitude (related to the area enclosed within PV contours). We interpreted this PV-gradient maximum as the transport barrier in the monsoon anticyclone. This PV-gradient based transport barrier for the monsoon is deducible in a layer around the tropopause (around 380 K) for most days between mid June to mid August 2011.

However, the PV-gradient based transport barrier, and hence the related confinement of air masses, in the monsoon anticyclone appears much weaker than the transport barrier at the edge of the polar vortex (e.g., Nash et al., 1996) and also weaker than the barrier at the subtropical jet (see Kunz et al., 2011), likely related to the large dynamic variability of the monsoon anticyclone. Daily maps of the anticyclone show large displacements in east-west direction, shedding of smaller-scale eddies and even splits (Fig. 10), frequently causing air masses to be torn out of the anticyclone. In particular the strong diabatic heating related to deep convection over South Asia affects the anticyclonic monsoon circulation (Randel and Park, 2006) and likely the strength of the transport barrier (e.g., Fig. 12). Hence, the anticyclone transport barrier turns out to be leaky, allowing cross-barrier transport to some degree, and the maximum PV gradient is better interpreted as a measure of confinement of the air masses than describing a rigid barrier to the flow. Nonetheless, for the sake of a clear terminology we used the term "barrier" throughout this study.

Despite the leakiness of the barrier, diagnosing the corre-

sponding PV-value offers a method to separate the core of the monsoon anticyclone from its surroundings. Hence, the size of the anticyclone core may be determined and air masses may be appropriately tagged. This offers new opportunities for model studies of Asian monsoon impact and for evaluation of measurements from the monsoon region. The degree of confinement inside the anticyclone further determines how effectively air masses from the anticyclone core mix with air from the anticyclone edge. Air masses from different transport pathways may be injected into different regions of the anticyclone (e.g., into the core by convection and upwelling within the conduit (Bergman et al., 2013), or into the anticyclone edge by taifoons over Southeast Asia (Vogel et al., 2014)). Therefore, chemical reactions and lifetimes of short-lived species, and the effectivity of pollution transport into the stratosphere will depend on the degree of confinement.

The smooth evolution of the anticyclone transport barrier over the season (Fig. 12) enhances our confidence in its relation to a physical mechanism. Furthermore, enhanced gradients in CLaMS simulated trace gas distributions (CO, O_3 and mean age) clearly demonstrate the existence of the PV-gradient based transport barrier. These enhanced trace gas gradients are reflected in corresponding minima in mixing ratio PDFs (see Appendix). However, a proper validation of the meaningfulness of the diagnosed transport barrier can only be achieved by comparison to trace gas measurements. Figure 14 compares the gradient of MLS observed ozone with respect to PV in the monsoon region to the PV-based transport barrier (grey symbols), similarly as in in Fig. 3 but for the entire season. Both reliably agree during beginning of July and middle to end of July. During mid of August, the PV-based barrier is located at higher PV values, but shows a similar temporal evolution as the maximum ozone gradient.

The disagreements between the model and MLS are not unexpected, mainly because of the different resolutions (e.g., vertical resolution around the tropopause of about 400 m in CLaMS versus about 3 km in MLS). Unfortunately, high-resolution in-situ observations from the Asian monsoon region are lacking. Current satellite observations are often affected by high clouds in this region, and their vertical resolution and horizontal spatial sampling is limited. Nonetheless, MLS ozone shows enhanced gradients coinciding with the PV value of the transport barrier during several days, providing further confidence in the PV-based anticyclone transport barrier. Further analysis of observations of sufficiently high resolution would be strongly desirable.

8 Conclusions

As shown by anomalies in several trace gas observations, the air inside the Asian monsoon anticyclone appears, at least to some degree, confined and isolated from its surroundings. Diagnosing the related transport barrier offers new opportunities for quantifying the transport of tropospheric source gases into the UTLS (e.g., determining anticyclone size, tagging air masses). In this paper, we showed that the potential vorticity field reflects the existence of a barrier to horizontal transport between the anticyclone and its surroundings. Although the detection of the transport barrier is hampered by the large dynamic variability of the anticyclone and the proximity to the subtropical jet a refined PV-gradient criterion may be used to deduce the barrier within the Asian monsoon anticyclone, in a layer around 380 K. Therefore, we refined the criterion developed for the polar vortex (e.g., Nash et al., 1996) and determine the anticyclone transport barrier from the PV-gradient maximum, after restricting the PV field to the monsoon region and averaging over a time window around the given date (summarized in Fig. 9). Comparison to simulated CO shows that the PV-gradient based transport barrier is meaningful in the sense of separating air masses of different chemical characteristics. The deduced PV values (e.g., 3.6 on average for 2011 at 380 K) offer a physically motivated criterion to separate the inner core of the anticyclone from the region around, crucial for the interpretation of trace gas observations and for model studies.

Appendix A Transport barrier from trace gas mixing ratio PDF

To further increase the confidence in the existence of the PV-gradient transport barrier, we deduce the anticyclone transport barrier also from simulated CO using a different methodology based on probability density functions (PDF) and show its consistency with the PV-based results (for a review of the PDF method, see Sparling, 2000). Therefore, we calculate the PDF of CLaMS simulated CO mixing ratios in the Asian monsoon region (10°-60°N, 10°W–160°E) for a ±1-day time window around 6 July 2011 (Fig. A1). The PDF was constructed after assigning the appropriate area-weighting to the data points. Mean CO monotonically decreases with increasing PV, with high CO inside the monsoon (coinciding with low PV) and low CO outside. Minima in the mixing ratio PDF indicate regions of suppressed horizontal transport (Sparling, 2000).

The PDF in Fig. A1 shows one minimum at CO mixing ratios around 35-40 ppbv, related to the subtropical jet, and a secondary minimum around 55 ppbv, related to the transport barrier inside the Asian monsoon anticyclone. From the PDF of PV values corresponding to CO mixing ratios around the minimum, we find a corresponding PV value of 4.1 PVU, in good agreement to the 4 PVU emerging from the PV-gradient maximum (Fig. A1/bottom).

For 6 July, the CO PDF shows the anticyclone transport barrier even for the instantaneous distribution, without averaging over ±1 days (not shown). Note that the PDF approach is related to the PV-gradient method (e.g., Neu et al., 2003; Palazzi et al., 2011). Still, the comparison between the two methods shows the robustness of the deduced transport bar-

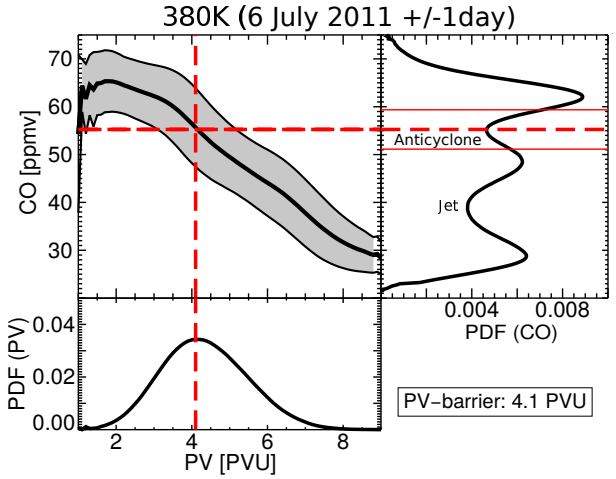

Fig. A1. Asian monsoon transport barrier at 380 K on 6 July 2011 from the CO mixing ratio PDF. The main panel (upper left) shows CLaMS CO (monsoon region average, 5–7 July time average) versus PV with one standard deviation as grey shading. The upper right panel shows the corresponding mixing ratio PDF with the monsoon transport barrier highlighted as red dashed line. The lower panel shows the PDF of PV-values around the barrier (between the thin red lines in the upper right panel). (See text for further details.)

rier. Similarly to the PV-based approach, the PDF approach fails in locating a transport barrier at several days during summer. The use of mixing ratio PDF's would offer a simple independent method to deduce the anticyclone transport barrier from satellite observations. Overall, the good agreement between the PV-gradient based, CO-gradient based and CO-PDF based approaches enhances our confidence in the physical meaningfulness of the deduced transport barrier estimates.

Acknowledgements. We thank Bernard Legras for advice, Nicole Thomas for programming support and the ECWMF for providing reanalysis data. F. Ploeger was funded by an HGF postdoc grant, and further thanks the HGF for supporting a research stay at the Laboratoire de Météorologie Dynamique of the École Normale Supérieure in Paris during which parts of this work had been carried out.

References

Abalos, M., Ploeger, F., Konopka, P., Randel, W. J., and Serrano, E.: Ozone seasonality above the tropical tropopause: reconciling the Eulerian and Lagrangian perspectives of transport processes, Atmos. Chem. Phys., 13, 10 787–10 794, 2013.

Bergman, J. W., Jensen, E. J., Pfister, L., and Yang, Q.: Seasonal differences of vertical-transport efficiency in the tropical tropopause layer: On the interplay between tropical deep convection, large-scale vertical ascent, and horizontal circulations, J. Geophys. Res., 117, D5, 2012.

Bergman, J. W., Fierli, F., Jensen, E. J., Honomichl, S., and Pan, L. L.: Boundary layer sources for the Asian anticyclone: Regional contributions to a vertical conduit, J. Geophys. Res., 118, 2560–2575, 2013.

Bian, J., Pan, L. L., Paulik, L., Vömel, H., Chen, H., and Lu, D.: In situ water vapor and ozone measurements in Lhasa and Kunming during the Asian summer monsoon, Geophys. Res. Lett., 39, doi: 10.1029/2012GL052996, 2012.

Butchart, N. and Remsberg, E. E.: The area of the stratospheric polar vortex as a diagnostic for tracer transport on an isentropic surface, J. Atmos. Sci., 43, 1319–1339, 1986.

Dee, D. P., Uppala, S. M., Simmons, A. J., Berrisford, P., Poli, P., Kobayashi, S., Andrae, U., Balmaseda, M. A., Balsamo, G., Bauer, P., Bechtold, P., Beljaars, A. C. M., van de Berg, L., Bidlot, J., Bormann, N., Delsol, C., Dragani, R., Fuentes, M., Geer, A. J., Haimberger, L., Healy, S. B., Hersbach, H., Holm, E. V., Isaksen, L., Kallberg, P., Kohler, M., Matricardi, M., McNally, A. P., Monge-Sanz, B. M., Morcrette, J. J., Park, B. K., Peubey, C., de Rosnay, P., Tavolato, C., Thepaut, J. N., and Vitart, F.: The ERA-Interim reanalysis: configuration and performance of the data assimilation system, Q. J. R. Meteorol. Soc., 137, 553–597, doi:10.1002/qj.828, 2011.

Fueglistaler, S., Dessler, A. E., Dunkerton, T. J., Folkins, I., Fu, Q., and Mote, P. W.: Tropical Tropopause layer, Rev. Geophys., 47, RG1004, doi:10.1029/2008RG000267., 2009.

Garny, H. and Randel, W. J.: Dynamic variability in the Asian monsoon anticyclone observed in potential vorticity and correlations with tracer distributions, J. Geophys. Res., 118, 13 421–13 433, 2013.

Gill, A. E.: Some simple solutions for heat-induced tropical circulation, Q. J. R. Meteorol. Soc., 106, 447–462, 1980.

Holton, J. R.: An Introduction to Dynamic Meteorology, Academic Press, London, 1992.

Hoor, P., Wernli, H., Hegglin, M. I., and Boenisch, H.: Transport timescales and tracer properties in the extratropical UTLS, Atmos. Chem. Phys., 10, 7929–7944, doi:10.5194/acp-10-7929-2010, 2010.

Hsu, C. J. and Plumb, R. A.: Non-axisymmetric thermally driven circulations and upper tropospheric monsoon dynamics, J. Atmos. Sci., 57, 12541276, 2000.

James, R., Bonazzola, M., Legras, B., Surbled, K., and Fueglistaler, S.: Water vapor transport and dehydration above convective outflow during Asian monsoon, Geophys. Res. Lett., 35, L20810, doi:10.1029/2008GL035441, 2008.

Konopka, P., Günther, G., Müller, R., dos Santos, F. H. S., Schiller, C., Ravegnani, F., Ulanovsky, A., Schlager, H., Volk, C. M., Viciani, S., Pan, L. L., McKenna, D.-S., and Riese, M.: Contribution of mixing to upward transport across the tropical tropopause layer (TTL), Atmos. Chem. Phys., 7, 3285–3308, 2007.

Konopka, P., Grooß, J. U., Günther, G., Ploeger, F., Pommrich, R., Müller, R., and Livesey, N.: Annual cycle of ozone at and above the tropical tropopause: observations versus simulations with the Chemical Lagrangian Model of the Stratosphere (CLaMS), Atmos. Chem. Phys., 10, 121–132, 2010.

Krishnamurti, T. N., Daggupaty, S. M., Fein, J., Kanamitsu, M., and Lee, J. D.: Tibetan high and upper tropospheric tropical circulation during Northern summer, Bull. Amer. Meteor. Soc., 54, 12341249, 1973.

Kunz, A., Konopka, P., Müller, R., and Pan, L. L.: Dynamical tropopause based on isentropic potential vorticity gradients, J. Geophys. Res., 116, D01110, 2011.

Kunze, M., Braesicke, P., Langematz, U., Stiller, G., Bekki, S., Brühl, C., Chipperfield, M., Dameris, M., Garcia, R., and Giorgetta, M.: Influences of the Indian summer monsoon on water vapor and ozone concentrations in the UTLS as simulated by chemistry-climate models, J. Climate, 23, 3525–3544, 2010.

Liebmann, B., and Smith, C. A.: Description of a complete (interpolated) outgoing longwave radiation dataset, Bull. Am. Meteorol. Soc., 77, 1275–1277, 1996.

Livesey, N. J., Filipiak, M. J., Froideveaux, L., Read, W. G., Lambert, A., Santee, M. L., Jiang, J. H., Pumphrey, H. C., Waters, J. W., Cofield, R. E., Cuddy, D. T., Daffer, W. H., Drouin, B. J., Fuller, R. A., Jarnot, R. F., Jiang, Y. B., Knosp, B. W., Li, Q. B., Perun, V. S., Schwartz, M. J., Snyder, W. J., Stek, P. C., Thurstans, R. P., Wagner, P. A., Avery, M., Browell, E. V., Cammas, J. P., Christensen, L. E., Diskin, G. S., Gao, R. S., Jost, H. J., Loewenstein, M., Lopez, J. D., Nedelec, P., Osterman, G. B., Sachse, G. W., and Webster, C. R.: Validation of Aura Microwave Limb Sounder O_3 and CO observations in the upper troposphere and lower stratosphere, J. Geophys. Res., 113, D15S02, doi:10.1029/2007JD008805, 2008.

Manney, G. L., Zurek, R. W., Gelman, M. E., Miller, A. J., and Nagatani, R.: The anomalous Arctic lower stratospheric polar vortex of 1992–1993, Geophys. Res. Lett.., 21, 2405–2408, 1994.

McKenna, D. S., Grooß, J.-U., Günther, G., Konopka, P., Müller, R., Carver, G., and Sasano, Y.: A new Chemical Lagrangian Model of the Stratosphere (CLaMS): 2. Formulation of chemistry scheme and initialization, J. Geophys. Res., 107, 4256, doi:10.1029/2000JD000113, 2002a.

McKenna, D. S., Konopka, P., Grooß, J.-U., Günther, G., Müller, R., Spang, R., Offermann, D., and Orsolini, Y.: A new Chemical Lagrangian Model of the Stratosphere (CLaMS): 1. Formulation of advection and mixing, J. Geophys. Res., 107, 4309, doi:10.1029/2000JD000114, 2002b.

Nash, E. R., Newman, P. A., Rosenfield, J. E., and Schoeberl, M. R.: An objective determination of the polar vortex using Ertel's potential vorticity, J. Geophys. Res., 101, 9471–9478, 1996.

Neu, J. L., Sparling, L. C., and Plumb, R. A.: Variability of the subtropical "edges" in the stratosphere, J. Geophys. Res., 108, doi:10.1029/2002JD002706, 2003.

Palazzi, E., Fierli, F., Stiller, G. P., and Urban, J.: Probability density functions of long-lived tracer observations from satellite in the subtropical barrier region: data intercomparison, Atmos. Chem. Phys., 11, 10 57910 598, doi:10.5194/acp-11-10579-2011, 2011.

Park, M., Randel, W. J., Gettelman, A., Massie, S. T., and Jiang, J. H.: Transport above the Asian summer monsoon anticyclone inferred from Aura Microwave Limb Sounder tracers, J. Geophys. Res., 112, D16309, doi:10.1029/2006JD008294, 2007.

Park, M., Randel, W. J., Emmons, L. K., Bernath, P. F., Walker, K. A., and Boone, C. D.: Chemical isolation in the Asian monsoon anticyclone observed in Atmospheric Chemistry Experiment (ACE-FTS) data, Atmos. Chem. Phys., 8, 757–764, 2008.

Ploeger, F., Konopka, P., Müller, R., Fueglistaler, S., Schmidt, T., Manners, J. C., Grooß, J.-U., Günther, G., Forster, P. M., and Riese, M.: Horizontal transport affecting trace gas seasonality in the Tropical Tropopause Layer TTL, J. Geophys. Res., 117, 09303, doi:10.1029/2011JD017267, 2012.

Ploeger, F., Günther, G., Konopka, P., Fueglistaler, S., Müller, R., Hoppe, C., Kunz, A., Spang, R., Grooß, J.-U., and Riese, M.: Horizontal water vapor transport in the lower stratosphere from subtropics to high latitudes during boreal summer, J. Geophys. Res., 118, 8111–8127, doi:10.1002/jgrd.5063, 2013.

Pommrich, R., Müller, R., Grooß, J.-U., Konopka, P., Ploeger, F., Vogel, B., Tao, M., Hoppe, C. M., Günther, G., Spelten, N., Hoffmann, L., Pumphrey, H.-C., Viciani, S., D'Amato, F., Volk, C. M., Hoor, P., Schlager, H., and Riese, M.: Tropical troposphere to stratosphere transport of carbon monoxide and long-lived trace species in the Chemical Lagrangian Model of the Stratosphere (CLaMS), Geosci. Model Dev., 7, 2895–2916, 2014.

Popovich, J. M. and Plumb, R. A.: Eddy Shedding from the Upper-Tropospheric Asian Monsoon Anticyclone, J. Atmos. Sci., 58, 93104, 2001.

Randel, W. J. and Park, M.: Deep convective influence on the Asian summer monsoon anticyclone and associated tracer variability observed with Atmospheric Infrared Sounder (AIRS), J. Geophys. Res., 111, D12314, doi:10.1029/2005JD006490, 2006.

Randel, W. J., Park, M., Emmons, L., Kinnison, D., Bernath, P., Walker, K. A., Boone, C., and Pumphrey, H.: Asian Monsoon Transport of Pollution to the Stratosphere, Science, 328, 611–613, doi:10.1126/science.1182274, 2010.

Sparling, L. C.: Statistical perspectives on stratospheric transport, Rev. Geophys., 38, 417–436, 2000.

Tzella, A. and Legras, B.: A Lagrangian view of convective sources for transport of air across the Tropical Tropopause Layer: distribution, times and the radiative influence of clouds, Atmos. Chem. Phys., 11, 12 51712 534, 2011.

Vogel, B., Günther, G., Müller, R., Grooß, J.-U., Hoor, P., Krämer, M., Müller, S., Zahn, A., and Riese, M.: Fast transport from Southeast Asia boundary layer sources to Northern Europe: Rapid uplift in typhoons and eastward eddy shedding of the Asian monsoon anticyclone, Atmos. Chem. Phys., 14, 12 745–12 762, 2014.

Waugh, D. W., and Hall, T. M.: Age of stratospheric air: Theory, observations, and models, Rev. Geophys., 40, 1–27, 2002.

WMO: Meteorology–A threedimensional science, WMO Bull, pp. 134–138, 1957.

Yan, R.-C., Bian, J.-C., and Fan, Q.-J.: The impact of the South Asia high bimodality on the chemical composition of the upper troposphere and lower stratosphere, Atmos. Oceanic Sci. Lett., 4, 220–234, 2011.

Zhang, Q., Wu, G., and Qian, Y.: The bimodality of the 100 hpa South Asia high and its relationship to the climate anomaly over East Asia in summer, J. Meteorol. Soc. Jpn., 80, 733–744, 2002.